THE PERKIN - ELMER CORPORATION
AEROSPACE SYSTEMS
2855 Metropolitan Place Pomona, California

A HIGH PRESSURE MAGNETIC ION SOURCE

Final Report

July 1967

NASA Contract Number
NAS 5-3453
Modification 6, Item R

Prepared for
NATIONAL AERONAUTICS AND SPACE ADMINISTRATION
Goddard Space Flight Center
Greenbelt, Maryland

ABSTRACT

A theoretical analysis developing the design equations for extending ion source operation to higher pressures has resulted in a test model capable of direct analysis of pressures up to 1×10^{-2} torr. Close agreement between the theory and the test results was obtained, and the operating pressure range of the test model was extended to 1×10^{-1} torr. The objective of the study was to produce a source capable of operation at 1×10^{-2} torr having a sensitivity of 1×10^{-8} amperes/torr without exceeding a time response of 0.030 seconds. Test of the instrument gave operation to 1×10^{-1} torr with a sensitivity of 8×10^{-9} amperes/torr. The time response was analyzed using a computer program, and for the defined interfacing system gave a response of .0025 seconds to 95% of a stepped pressure change.

TABLE OF CONTENTS

LIST OF SYMBOLS

Q_o	=	Net inlet gas flow (torr - liters/second)
Q_s	=	Net source gas flow (torr - liters/second)
Q_a	=	Net analyzer gas flow (torr - liters/second)
C_o	=	Inlet gas conductance (liters/second)
C_s	=	Ion source gas conductance (liters/second)
C_a	=	Analyzer gas conductance (liters/second)
S_p	=	Pumping speed (liters/second)
V_s	=	Ion source volume (liters)
V_a	=	Analyzer volume (liters)
P_o	=	External sample gas pressure (torr)
P_s	=	Ion source maximum design pressure (torr)
P_a	=	Analyzer pressure (torr)
P_p	=	Pump pressure (torr)
D	=	Differential pumping ratio, P_s/P_a (dimensionless)
C_1	=	Ion exit aperture conductance (liters/second)
C_2	=	Electron entrance aperture conductance (liters/second)
α_1	=	Correction factor for length to diameter ratio for ion exit aperture conductance (dimensionless)
K	=	Correction factor for length to height ratio for electron entrance aperture conductance (dimensionless)
L_1	=	Ion exit aperture length (meters)
R	=	Ion exit aperture radius (meters)

L_2 = Electron entrance aperture length (meters)

w = Electron entrance aperture width (meters)

t = Electron entrance aperture height (meters)

λ_{gas} = Mean free path of the gas species (meters)

λ_e = Mean free path of the electrons in the gas species (meters)

λ_i = Mean free path of the ions in the gas species (meters)

ℓ_1 = Electron beam path length in ionizing region (meters)

ℓ_2 = Ion beam path length in ionizing region (meters)

t' = Thickness of electron beam (meters)

d = Distance separating ion extraction electrodes (meters)

a = Fraction of distance separating ion extraction electrodes from the accelerator at which the electron beam is located (dimensionless)

I_o^- = Initial electron current entering ionizing region (amperes)

I_{AN}^- = Electron current reaching anode (amperes)

I_i^- = Electron current at point where ions are extracted (amperes)

I_o^+ = Initial ion current formed by I_i^- (amperes)

I^+ = Ion current reaching ion exit aperture (amperes)

I_F^+ = Total ion current formed (amperes)

I_T^+ = Total transmittable ion current (amperes)

J^- = Electron current density (amperes/meter^2)

S = Ionization cross-section $\left[I_F^+ \text{ (amperes)}/I^- \text{(amperes - torr - meter of electron path length}\right]$

P_c = Critical pressure (torr)

x = Ion source pressure to critical pressure ratio (dimensionless)

i_v = Ionizing electron current to ion extraction potential ratio (micro-amperes/volt)

α_2 = Ionizing plane potential to ion extraction potential ratio (dimensionless)

ϵ_o = Permittivity of free space (8.85×10^{-12} farads/meter)

e = Electronic charge (1.6×10^{-19} coulombs)

m_e = Mass of electron (kilograms)

M = Mass of positive ion (kilograms)

V_r = Ion extraction (repeller) potential (volts)

ΔV_{ion} = Ion energy spread (volts)

V_{el} = Energy of ionizing electrons (volts)

v_e = Electron beam velocity through ionizing region (meters/second)

B_z = Flux density of electron beam aligning magnetic field (webers/meter^2)

θ = Walking angle of magnetically aligned electron beam in the ion extraction field (°)

$I^+_{SC}\Big|_{\substack{TUN\\MAX}}$ = Space charge limit of ion current transmittable through a tunnel aperture (amperes)

$I^-_{SC}\Big|_{\substack{TUN\\MAX}}$ = Space charge limit of electron current transmittable through a tunnel aperture when magnetically aligned (amperes)

$V_{el}\Big|_{APERTURE}$ = Electron energy upon reaching electron entrance aperture (volts)

τ_s = Ion source time constant (seconds)

1. INTRODUCTION

The primary function of a mass spectrometer system is to analyze a gaseous mixture, separate the components of the mixture, and measure the resulting partial pressures of the constituents. This procedure is accomplished by four interrelated system components as described below:

a. A sample gas inlet system which conducts a portion of the gas from the area to be analyzed to the ion source.

b. An ion source to create positive ions of the various species, the quantities of which are directly proportional to the partial pressures of the gas constituents, and then focuses the ions into the analyzer section.

c. An analyzer which can separate, or filter, the ions according to their mass to charge ratios, m/e's, and pass them into a collector, or collectors, from which they may be detected.

d. A detector to measure the ion currents which strike the collecting system, and read out a signal corresponding to the partial pressures which are present.

The ion source is thus a critical point of the system, since it is here that the change in regime takes place, being the conversion of the neutral atomic or molecular species to ions proportional to the partial pressures of the gases present in the mixture. However, all ion sources presently being produced have upper pressure limitations, the highest of which operate up to approximately 1×10^{-3} torr. Consequently, when sampling pressures higher than this level, a pressure dividing network is required in the inlet system in order to reduce the sample pressure to an acceptable level to insure proper operation of the ion source.

In a space flight mass spectrometer system designed to sample an atmosphere from a spacecraft at higher pressure levels than the ion source upper pressure limitations, a direct leak is generally employed as the inlet system between the external atmosphere and the ion source. This is done to obtain the proper pressure differential required. This restriction in the gas flow then imposes a time constant in the inlet line, such that the smaller the leak, corresponding to higher external pressures, the longer becomes the time response of the mass spectrometer system. In a laboratory instrument instrument in which the external pressure of the sample is maintained, this effect does not cause problems. But, in a spacecraft moving through a changing atmospheric density at a relatively high velocity, the time response of the instrument becomes a critical factor in measuring constituent partial pressures as a function of the spacecraft altitude.

The problem presented is thus to build an ion source such that a space flight mass spectrometer system is capable of analyzing relatively high external pressures, and with a very low time response so that timely and meaningful data can be obtained of the atmospheric density. To reduce the inlet system time constant, the pressure differential across the leak must be reduced; which means that the ion source to be used must be capable of withstanding operation at higher pressure levels.

2. TASK DEFINITION AND GOALS

The purpose of this study was to perform a theoretical investigation of a high pressure ion source, utilizing a magnetically aligned electron beam, and to perform the mechanical design, fabrication, and testing of the ion source having the following design goals:

a. The capability of matching a previously designed mass spectrometer while providing a sensitivity approaching 1×10^{-8} amperes/torr.

b. An upper operating pressure limitation of 1×10^{-2} torr.

c. A maximum ion source time response of 30 milliseconds.

Other important characteristics to be inherent with the design were the stability and linearity over the operating pressure range, and interchangibility with the ion sources previously manufactured as part of the specialized mass spectrometer systems built under Contract NAS5-3453.

3. THEORETICAL ANALYSES AND CONSIDERATIONS

3.1 GAS FLOW CONSIDERATIONS

To design an ion source capable of high pressure operations, the first consideration becomes a question of the maximum allowable pressure in the analyzer to which the ion source will be fitted, and whether or not a vacuum pump will be fitted to the instrument. If the analyzer pressure is much lower than that of the ion source, then gas restricting apertures must be placed between the ionizing region and the analyzer to create the required pressure differential. At high pressures the use of this pressure differential becomes extremely important due to the effect upon the mean free paths of the ions formed.

The gas flow through the entire mass spectrometer system can be defined in terms of the variables shown in Figure 3-1a if a vacuum pump is used, or as in Figure 3-1b without a vacuum pump but using the evacuated volume of the analyzer as a vacuum capacity.

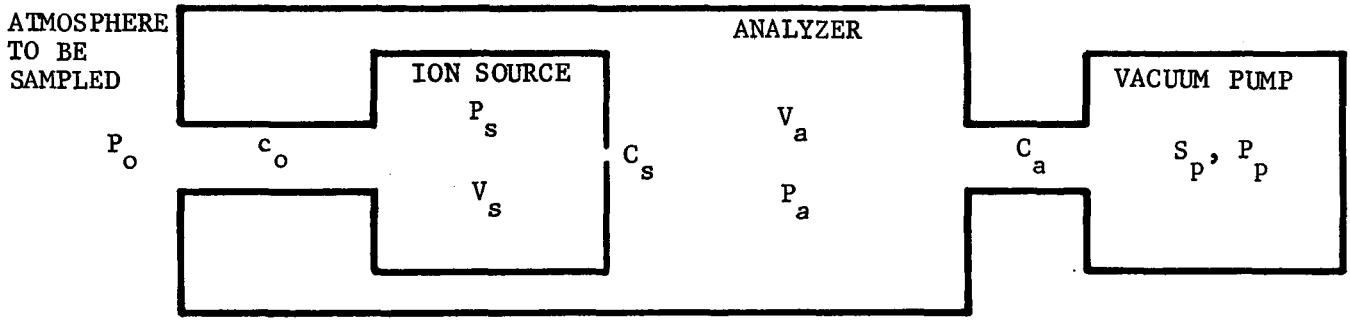

FIGURE 3-1a

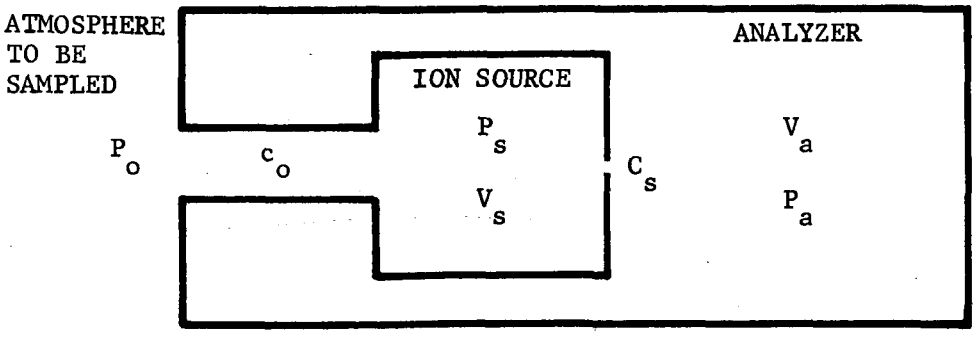

FIGURE 3-1b

Under changing conditions, if we differentiate the energy (PV) of the gas contained in the analyzer volume;

$$\frac{d(PV)}{dt} = Q_E = P\frac{dV}{dt} + V\frac{dP}{dt} = \text{Energy flow.}$$

At equilibrium pressure, as in Figure 3-1a, $\frac{dP}{dt} = 0$ and $\frac{dV}{dt} = S$, the pumping speed of the attached pump. Thus,

$$Q_E = PS \tag{3-1}$$

Without a pump, $\frac{dV}{dt} = 0$ and

$$Q_E = V_a \frac{dP_a}{dt} \tag{3-2}$$

for the analyzer volume.

The flow into the analyzer volume from Figure 3-1b can be expressed also as

$$Q_E = C\Delta P = C_s(P_s - P_a)$$

Equating with (3-2),

$$\frac{dP_a}{dt} = \frac{C_s(P_s - P_a)}{V} \tag{3-3}$$

Integrating,

$$P_a = P_s\left[1 - e^{-C_s/V}\right] \quad . \tag{3-4}$$

3.1.1 SYSTEM WITH A PUMP ATTACHED

Considering now, the more general system, with a vacuum pump attached, the gas flow can be described as follows:

$$Q_o = C_o(P_o - P_s) \qquad \text{(a)}$$

$$Q_s = C_s(P_s - P_a) \qquad \text{(b)} \tag{3-5}$$

$$Q_a = C_a(P_a - P_p) = P_p S_p \qquad \text{(c)}$$

The ion source changes in pressure as a function of time can then be written the general form of (3-3) as

$$\frac{dP_s}{dt} = \frac{1}{V_s}\left[(P_o - P_s)C_o - (P_s - P_a)C_s\right]$$

or

$$\frac{dP_s}{dt} = \frac{1}{V_s}\left[P_oC_o - (C_o + C_s)P_s + P_aC_s\right], \qquad (3\text{-}6)$$

and the change in the analyzer pressure with time is expressed by

$$\frac{dP_a}{dt} = \frac{1}{V_a}\left[(P_s - P_a)C_s - (P_a - P_p)C_a\right]$$

$$= \frac{1}{V_a}\left[(P_s - P_a)C_s - P_pS_p\right] . \qquad (3\text{-}7)$$

But

$$S_pP_p = (P_a - P_p)C_a$$

or

$$P_p = \left(\frac{C_a}{S_p + C_a}\right)P_a ,$$

and substituting in Equation (3-7) for P_p gives

$$\frac{dP_a}{dt} = \frac{1}{V_a}\left[P_sC_s - \left(C_s + \frac{C_aS_p}{S_p + C_a}\right)P_a\right] \qquad (3\text{-}8)$$

In the condition where equilibrium has been reached by the system with a constant surrounding atmosphere, then the flow into the analyzer is equal to the flow out, or

$$Q_s = Q_a = C_s(P_s - P_a) = S_pP_p$$

Also from (3-5b and c) the differential pumping ratio of the source can be written

$$D = \frac{P_s}{P_a} = 1 + \left(\frac{S_p}{C_s}\right)\left(\frac{C_a}{S_p + C_a}\right) \qquad (3\text{-}9)$$

and thus, for

$$C_a \gg S_p \; ; \quad D \approx 1 + \frac{S_p}{C_s} \quad \text{and} \quad Q_a \approx S_p P_a$$

$$C_a = S_p \; ; \quad D = 1 + \frac{S_p}{2C_s} \quad \text{and} \quad Q_a = \frac{1}{2} S_p P_a$$

$$C_a \ll S_p \; ; \quad D \approx 1 + \frac{C_a}{C_s} \quad \text{and} \quad Q_a \approx C_a P_a$$

This shows that it is desirable to make C_s small and S_p and C_a large to achieve a large differential pumping. A large or comparable C_a relative to S_p will save power and weight of the pump.

3.1.2 SYSTEM WITHOUT A PUMP

In the system without a vacuum pump attached to the analyzer, the gas flow is described by the following:

$$Q_o = C_o(P_o - P_s) \tag{3-10}$$

$$Q_s = C_s(P_s - P_a) \tag{3-11}$$

$$Q_a = C_s(P_a - P_s) \tag{3-12}$$

Changes in the ion source pressure as a function of time are thus represented by

$$\frac{dP_s}{dt} = \frac{1}{V_s}\left[P_o C_o - (C_o + C_s)P_s + P_a C_s\right] \; . \tag{3-13}$$

The change in the analyzer pressure with time is:

$$\frac{dP_a}{dt} = \frac{C_s}{V_a}\left[P_s - P_a\right] \; . \tag{3-14}$$

It is then obvious that at equilibrium, i.e., when the gas flow into the analyzer equals the flow out, that the analyzer pressure will be equal to the ion source pressure such that

$$D = \frac{P_s}{P_a} = 1 \tag{3-15}$$

However, in an actual case the flight path of the space vehicle from which measurements are taken must be known so that the pressure in the ion source and analyzer can be computed. The effective differential pumping is a function of time as described by Equations (3-13) and (3-14) for an assumed and fixed external pressure. Some estimates of accumulated pressure can be determined from these equations.

3.1.3 GAS FLOW THROUGH APERTURES

The gas conductances defined previously in Figures 3-1a and 3-1b can be controlled by the use of restricting apertures which can limit the flow. The determination of the gas flow through annular and rectangular apertures can be computed from the dimensions of the holes by use of the relationships given by Guthrie and Wakerling.[1] They give the expression for the conductance of a short round pipe as

$$C = \left[\frac{\pi}{3}\sqrt{\frac{kT}{2\pi M}}\,\frac{(2R)^3}{L_1}\right]\alpha_1 \qquad (3\text{-}16)$$

which for air at 20°C becomes

$$C = 12.1\,\frac{(2R)^3}{L_1}\,\alpha_1 \quad \text{(liters/second)} \qquad (3\text{-}17)$$

where the values for α_1 are tabulated in Table 3-1, and where R and L_1 are expressed in centimeters.

TABLE 3-1

$L_1/2R$	α_1
0.05	0.036
0.08	0.055
0.1	0.068
0.2	0.13
0.4	0.21
0.6	0.28
0.8	0.30
1.0	0.38
2	0.54
4	0.70
6	0.77
8	0.81
10	0.84
20	0.91
40	0.95
60	0.97
80	0.98
≥100	1

For a long thin slitlike tube, where t is the height, w the width and of length L_2 in centimeters, the conductance is expressed by

$$C = 30.9 \frac{wt^2}{L_2} K \quad \text{(liters/second)} \tag{3-18}$$

for air at 20°C. For a short thin slitlike tube, this expression becomes modified by the aperture conductance (as with the α_1 factor in the round tube) where the total conductance through the slit is then

$$C = \frac{C_{SLIT}\, C_{AP}}{C_{SLIT} + C_{AP}} \tag{3-19}$$

The aperture conductance is found by

$$C_{AP} = 11.6 \frac{AA_o}{A_o - A} \tag{3-20}$$

where

A = area of the aperture (cm^2)

A_o = area of the region from which the gas flows (cm^2).

For $A_o \gg A$, this becomes

$$C_{AP} = 11.6\, A \tag{3-21}$$

The values of K are tabulated in Table 3-2.

TABLE 3-2

L_2/t	K
0.1	0.036
0.2	0.068
0.4	0.13
0.8	0.22
1	0.26
2	0.40
3	0.52
4	0.60
5	0.67
10	0.94
>10	$\frac{3}{8} \ln\left(\frac{L_2}{t}\right)$

For the circular aperture condition, it is seen that a_1 is dependent upon the length to diameter ratio, $L_1/2R$, so that it is convenient to rewrite Equation (3-17) for dimensions in MKS units in the following form,

$$C = 48.4 \times 10^4 R^2 \left(\frac{2R}{L_1}\right) a_1 \quad \text{(liters/second)} \quad . \tag{3-22}$$

Similarly, since K is dependent upon the length to height ratio, L_2/t_1 with the slitlike tube, Equation (3-18) becomes

$$C = 30.9 \times 10^4 \, wt \left(\frac{t}{L_2}\right) K \quad \text{(liters/second)} \tag{3-23}$$

and the aperture conductance is then

$$C_{AP} = 11.6 \times 10^4 \frac{AA_o}{A_o - A} \quad \text{(liters/second)} \tag{3-24}$$

where the areas are now expressed in square meters.

3.1.4 DIFFERENTIAL PUMPING

Due to mean-free-path considerations, a high pressure source must be small in size. However, it is only necessary to maintain the ionizing region at the elevated pressure level. Consequently, the filament and electron gun can be kept at the analyzer pressure level. The advantages of this type of system are threefold:

a. Sample distortion due to interaction of the sample with the filament is reduced, the most important being the conversion of O_2 to CO thereby reducing the m/e 32 peak and increasing the m/e 28 peak.

b. Space charge effects are minimized in the electron focusing system when it is external to the high pressure region, thus giving greater stability of the emission system.

c. In a system utilizing a vacuum pump, a minimal degree of preferential gas pumping is created by the pump. This avoids building up a large partial pressure of a gas having relatively low pumping speed.

It is desirable in the design of a high pressure ion source to limit the gas flow out of the ionizing region. Using the design discussed above, two places are required; the electron entrance aperture through which the ionizing electron beam is focused, and the ion exit aperture from which the ions are conducted to the analyzer region. For a high pressure instrument, it is desirable to place the ion exit restriction between the ionizing region and the ion focusing area. This allows for minimal travel of the ions within the high pressure region, and reduces the effective volume of the source.

3.1.5 ELECTRON GUN - IONIZING REGION - ANALYZER INTERFACING

The electron guns found most suitable for stability in space-flight applications have consisted of straight wire filaments of small diameter which are spring loaded. By this method of operation, the hot spot of the filament becomes aligned with the focusing system. This implies that the electron emission will be a beam having a width along the wire surface and a height related to the wire diameter.

The analyzer of the Specialized Mass Spectrometer toward which this study is projected consists of a quadrupole mass filter designed to accept ions having:

a. Energies up to 300 ev.

b. Energy spreads up to 15 ev.

c. Entrance angles up to 1.3° emerging from a circular aperture having a diameter of 0.010 inches (2.54×10^{-4} meters).

This analyzer can be provided with a vacuum pump, and this is assumed here.

Interfacing the ion source to the analyzer and the filament then defines the shapes of the ionizing region apertures. A circular ion exit aperture from the ionizing region allows for the symetrical x and y transmission of the ions while limiting the conductance of the hole to a minimum. At the electron entrance aperture, a thin slitlike tube becomes the most efficient type of aperture, giving the best current density while keeping the beam thickness small. This configuration also provides a low ion energy spread, as is later shown to be important and a beam wider than the diameter of the ion aperture. Consequently misalignment of the electron beam over this hole will not degrade the performance of the source.

3.1.6 APERTURE DEPENDENCE UPON PRESSURE

From the foregoing discussion, it is apparent that the ion source gas flow can be expressed by

$$C_s = C_1 + C_2$$

where C_1 and C_2 represent the conductances of a round hole and rectangular slit respectively. Letting

$$C_s = K_1 C_1 \quad , \tag{3-25}$$

where

$$K_1 = 1 + \frac{C_2}{C_1} \quad ,$$

and substituting Equation (3-22) for C_1, it is seen that

$$C_s = 48.4 \times 10^4 \, K_1 R^2 \left(\frac{2R}{L_1}\right) a_1 \quad . \tag{3-26}$$

The ion source pressure can then be defined in terms of conductances by substituting Equation (3-26) for C_s into Equation (3-9), which gives

$$P_s = P_a \left[1 + \frac{S_p}{48.4 \times 10^4 K_1 R^2 \alpha_1} \left(\frac{L_1}{2R} \right) \right] \left[\frac{C_a}{S_p + C_a} \right] \quad . \tag{3-27}$$

By making the assumption that $C_a \gg S_p$

$$P_s = P_a \left[1 + \frac{S_p}{48.4 \times 10^4 K_1 R^2 \alpha_1} \left(\frac{L_1}{2R} \right) \right] \tag{3-28}$$

However, since α_1 is dependent upon the $L_1/2R$ ratio, it is convenient to write

$$K_2 = \left(\frac{L_1}{2R} \right) \left(\frac{1}{\alpha_1} \right) \tag{3-29}$$

where L_1/R and α_1 are held constant. From Equations (3-28) and (3-29) the ion exit aperture radius can then be described by

$$R = \left[\frac{K_2 S_p}{48.4 \times 10^4 K_1} \right]^{1/2} \left[\frac{P_s}{P_a} - 1 \right]^{-1/2} \quad . \tag{3-30}$$

However, for the large differential pumping ratios assumed here, then $P_s/P_a \gg 1$, and this equation reduces to the form

$$R = \left[\frac{K_2 S_p P_a}{48.4 \times 10^4 K_1} \right]^{1/2} P_s^{-1/2} \quad . \tag{3-31}$$

Here the radius defines both source apertures through the constant K_1 and is, itself, defined by the design pressures.

3.2 IONIZING REGION PARAMETER CONSIDERATIONS

An objective in the design of any ion source is generally one of obtaining the maximum ion source sensitivity for a given electron current density without sacrificing the linearity or stability of the instrument. In a high pressure application, many of the parameters assume a much higher degree of importance than in lower pressure instruments where they may be considered negligible. Consequently, this investigation assumes a more complete approach toward all of the variables involved. Each of these parameters are covered in the sections below, and the interrelationships between them are explained.

Figure 3-2 illustrates a model of the ionizing region with the primary variables defined. The theoretical analysis that follows is based upon this model.

In the process of optimizing an ion source design, not only the pressure and current are variables but also all of the other parameters, such as the dimensions, are considered to be variables. Consequently, in the work that follows these parameters are scaled larger and smaller with other variables until the configuration appears to operate correctly in the desired pressure range.

3.2.1 CHARGED PARTICLE COLLISIONS WITH THE GAS

The motion of a neutral gas molecule is such that the particle will travel along a straight path until it either collides with another particle or with one of the walls of the containing vessel. The same condition is true for a charged particle with the exception that it may undergo deflections by electrostatic or magnetic fields. The mean distance traveled between these collisions is the mean free path of the particle. This mean free path is given by

$$\lambda_{gas} = \frac{kT}{\sqrt{2}\pi\sigma^2} P^{-1} \quad . \tag{3-32}$$

For low-velocity electrons, such as obtained in the use of an ionization gauge, Cobine[2] gives the mean free path for electrons as

$$\lambda_e = 4(2)^{1/2} \lambda_{gas} = \frac{K_4}{P} \tag{3-33}$$

and for ions as

$$\lambda_i = (2)^{1/2} \lambda_{gas} \quad . \tag{3-34}$$

For stable ion source operation, it is desirable to be able to regulate the electron beam current passing through the ionizing region such that the ion current generated will be solely a function of the pressure. It is assumed here that this is accomplished by collection on an anode beyond the ionizing region. Space charge will also affect this ion current as shown later.

To obtain linearity of the ion current with pressure it is normally necessary to operate in a low pressure regime such that a high percentage of this current is transmitted to the exit slit. A self-compensating method is used here to extend the linearity to higher pressures.

From Beer-Lambert's law, the transmission of any charged particles can be expressed by

$$\frac{I}{I_o} = e^{-\ell/\lambda} \quad . \tag{3-35}$$

Rewriting this expression gives the path length required for a set percentage transmission of current as,

$$\ell = \lambda \ln\left(\frac{I_o}{I}\right) \quad . \tag{3-36}$$

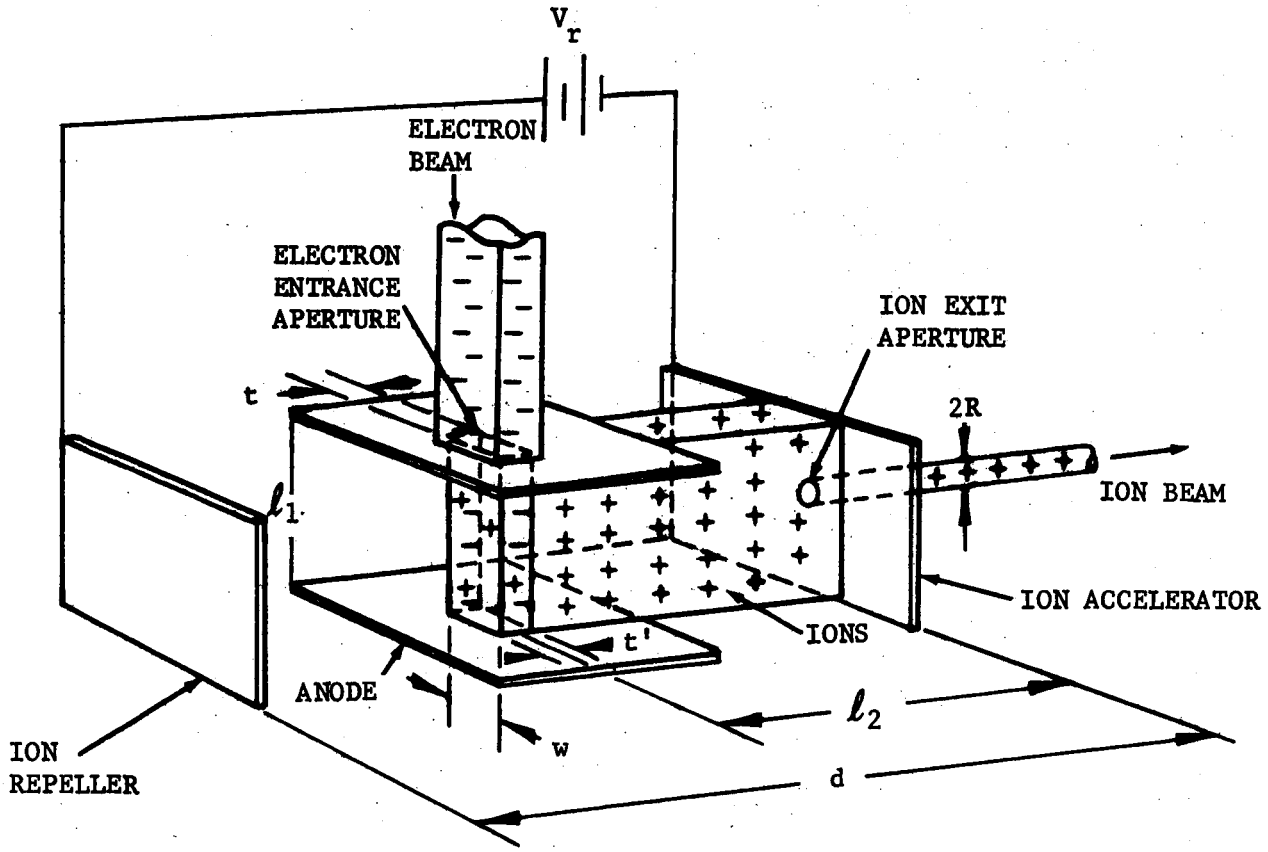

FIGURE 3-2
Model of the Ionizing Regions

For an air sample, the path length of the electron beam through the high pressure region of the source is then

$$\ell_1 = \frac{1}{P_s}\left[2.75 \times 10^{-4} \ln\left(\frac{I_o^-}{I^-}\right)\right] \text{ (meters)}, \tag{3-37}$$

and for the ion beam formed becomes

$$\ell_2 = \frac{1}{P_s}\left[6.87 \times 10^{-5} \ln\left(\frac{I_o^+}{I^+}\right)\right] \text{ (meters)}. \tag{3-38}$$

One feature which can be extracted from these equations is the fact that a geometrical relationship can be formed between these two path lengths. First, assume the aperture through which the ions are extracted is placed at some fraction, K_3, of the entrance-anode electron beam path length, ℓ_1. The current passing over the entire path length and reaching the anode, I_{AN}^-, of the source can be described by

$$I_{AN}^- = I_o^- e^{-\ell_1/\lambda_e}, \tag{3-39}$$

and the electron current forming the ions to be extracted through the aperture is expressed by

$$I_i^- = I_o^- e^{-K_3\ell_1/\lambda_e}. \tag{3-40}$$

Eliminating the initial electron current gives the expression

$$I_i^- = I_{AN}^- e^{[-\ell_1/\lambda_e](1-K_3)}. \tag{3-41}$$

Rewriting Equation (3-35) for the ion current at the exit of the high pressure region gives

$$I^+ = I_o^+ e^{-\ell_2/\lambda_i}. \tag{3-42}$$

But the ion current formed, I_o^+, can also be described by

$$I_o^+ = K'I^- \tag{3-43}$$

Where

K' = a constant involving the ionization cross section, the source pressure, the electron current density, and volume from which the ions are extracted.

Combining Equations (3-41), (3-42), and (3-43), the ion current at the exit aperture is thus

$$I^+ = K'I^-_{AN} \; e^{\left[\frac{\ell_1}{\lambda_e}(1-K_3) - \frac{\ell_2}{\lambda_i}\right]} \quad . \tag{3-44}$$

However, if regulation of the ionizing electron current is accomplished by keeping the anode current constant, then the transmittable ion current can be made independent of the mean free path of the ions only if the exponent of Equation (3-44) is set equal to 0, from which the following distance relationship can be given as

$$\frac{\ell_2}{\ell_1} = \frac{\lambda_i}{\lambda_e}(1-K_3) \quad . \tag{3-45}$$

Replacing λ_i and λ_e by their equivalents in Equations (3-33) and (3-34) gives

$$\frac{\ell_2}{\ell_1} = \frac{1}{4}(1-K_3) \tag{3-46}$$

While this expression gives a geometrical relationship between the path lengths of the electron and ion beams, it is believed that the uncertainties in the exact values of the mean free paths are such that the use of this formula would be helpful over a limited range of ion current transmission. Another limitation on this equation would also be the maximum amount of electron current which can be generated before filament failure.

3.2.2 SPACE CHARGE LIMITATIONS

The ion current formed within the ionizing region of an ion source is described by the equation

$$I^+_F = SJ^-P_s \, wt'\ell_1 \quad , \tag{3-47}$$

or a density facing the ion aperture of

$$J^+_F = SJ^-P_s \, t' \quad ,$$

for an electron beam of length ℓ_1 in the ionizing region and a cross sectional area of wt'. The transmittable ion current is then dependent upon the area of the ion exit aperture. Assuming a circular aperture of radius R as determined by Equation (3-31), this current is then expressed by

$$I^+_T = \pi SJ^-P_s \, t'R^2 \quad . \tag{3-48}$$

However, the presence of an electron beam and ion formation will create a change in the space potential where the ionization is taking place. With the electron beam current held constant, the space potential, in general, will change with the pressure due to an unbalanced change in charge within the region. The influence of this space charge in the ionizing region has been examined by Brubaker.[3] He defines the ion source pressure as a fraction, x, of a quantity termed the critical pressure, which is the pressure at which the potential of the ionizing plane becomes independent of the electron current density. Thus the expression is:

$$P_s = xP_c \quad , \tag{3-49}$$

where the critical pressure is described by

$$P_c = \left(\frac{3}{4dS}\right)\left(\frac{V_r m_e}{aV_{el}M}\right)^{1/2} \quad , \tag{3-50}$$

where

d = Spacing, repeller to accelerator (meters)

a = Fractional spacing of electron beam

S = Ionization coefficient (ions/electron - meter of path length torr pressure)

V_R, V_{el} = Potentials of repeller and electrons (volts)

m_e, M = Masses of the electron and ion (kilogram).

It is then convenient to define normalized quantities of the anode current and the potential of the ionizing plane with respect to the ion extraction potential, giving

$$i_v = \left(\frac{\bar{J}wt'}{V_r}\right)(10^6) \ (\mu\text{amp/volt}) \tag{3-51}$$

where $\bar{J}$, w and t' are density, width and thickness of the electron beam, respectively. Also defined is

$$\alpha_2 = \frac{V_{\text{IONIZING PLANE}}}{V_r} \quad . \tag{3-52}$$

He then derives an expression for α_2 as a function of space charge when i_v is small such that

$$\alpha_2 = a\left[1 + Ai_v\,(x - 1)\right] \quad , \tag{3-53}$$

where

$$A = \frac{(1-a)d \times 10^{-6}}{\epsilon_o w} \left(\frac{m_e}{2V_{el}e}\right)^{1/2} .$$

Figure 3-3 is then a plot of the potential of ionizing plane versus the anode current, each of which is normalized with respect to the ion extraction potential, V_r using x as a parameter.

Substituting for P_s and J^-, from Equations (3-49), (3-50), and (3-51) into (3-48) the transmittable ion current is then described by

$$I_T^+ = \left(\frac{3}{4} \times 10^{-6}\right)\left(\frac{m_e}{aV_{el}M}\right)^{1/2} (i_v x)\left(\frac{R^2}{wd}\right) V_r^{3/2} \qquad (3\text{-}54)$$

The maximum transmittable ion current is now defined in terms of the dimensions of the source and the space-charge parameters, i_v and x. Choice of values for i_v and x will determine the amount of each sign of space-charge present and the degree of non-linearities in operation that are allowed.

It is also apparent that, from this equation alone, ion source size does not control the ion current, if all dimensions scale together. However, the applied repeller potential has a strong influence. Limitations toward increasing V_r occur due to increased deflection of the electron beam and increased ion energy spread.

The distance from the ionizing plane to the ion exit aperture, a · d, is equal to the previously defined distance, ℓ_2, or from Equation (3-46)

$$ad = \ell_2 = \frac{\ell_1}{4}(1 - K_3) \quad . \qquad (3\text{-}55)$$

From Equations (3-39) and (3-33), and eliminating ℓ_1, then

$$d = \frac{\ell_2}{a} = \left(\frac{1-K_3}{4a}\right)\left[K_4 \ln\left(\frac{I_o^-}{I_{AN}^-}\right)\right] P_s^{-1} \qquad (3\text{-}56)$$

where

$$K_4 = 4(2)^{1/2} \lambda_{gas} P_s$$

The gas mean-free-paths are tabulated for various gases in Table 3-3.

The ion extraction potential, V_r, can also be written in terms of the ion source pressure by combining Equations (3-49) and (3-50), and by rearranging the terms to give

$$V_r = \left(\frac{4dS}{3x}\right)^2 \left(\frac{aV_{el}M}{m_e}\right) P_s^2 \qquad (3\text{-}57)$$

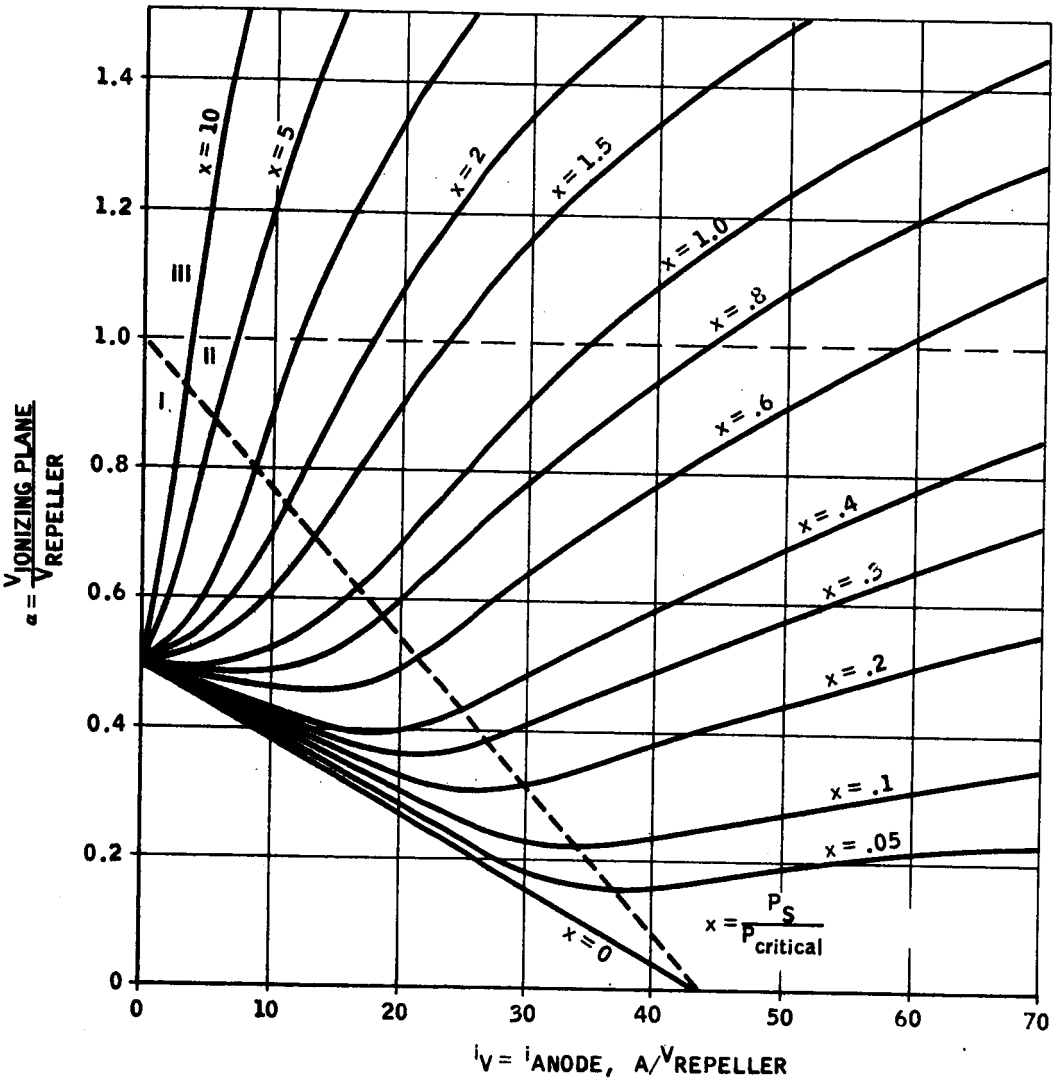
1.4
1.2
1.0
0.8
0.6
0.4
0.2
0
0
10
20
30
40
50
60
70
x = 10
x = 5
x = 2
x = 1.5
x = 1.0
x = .8
x = .6
x = .4
x = .3
x = .2
x = .1
x = .05
x = 0
III
II
I
$\alpha = \frac{V_{IONIZING\ PLANE}}{V_{REPELLER}}$
$x = \frac{P_S}{P_{critical}}$
$i_V = i_{ANODE,\ A}/V_{REPELLER}$

FIGURE 3-3

TABLE 3-3

Gas	λ_{gas} (meters)	λ_e (meters)	K_4 (torr-meters)	λ_i (meters)
H_2	$8.97\times10^{-5}/P$	$5.08\times10^{-4}/P$	5.08×10^{-4}	$1.27\times10^{-4}/P$
He	$1.41\times10^{-4}/P$	$7.99\times10^{-4}/P$	7.99×10^{-4}	$1.99\times10^{-4}/P$
CH_4	$3.92\times10^{-5}/P$	$2.22\times10^{-4}/P$	2.22×10^{-4}	$5.55\times10^{-5}/P$
NH_3	$3.42\times10^{-5}/P$	$1.94\times10^{-4}/P$	1.94×10^{-4}	$4.84\times10^{-5}/P$
H_2O vapor	$3.18\times10^{-5}/P$	$1.80\times10^{-4}/P$	1.80×10^{-4}	$4.50\times10^{-5}/P$
Ne	$1.00\times10^{-4}/P$	$5.66\times10^{-4}/P$	5.66×10^{-4}	$1.41\times10^{-4}/P$
N_2	$4.77\times10^{-5}/P$	$2.70\times10^{-4}/P$	2.70×10^{-4}	$6.75\times10^{-5}/P$
Air	$4.86\times10^{-5}/P$	$2.75\times10^{-4}/P$	2.75×10^{-4}	$6.87\times10^{-5}/P$
O_2	$5.15\times10^{-5}/P$	$2.92\times10^{-4}/P$	2.92×10^{-4}	$7.29\times10^{-5}/P$
HCl	$3.38\times10^{-5}/P$	$1.91\times10^{-4}/P$	1.91×10^{-4}	$4.78\times10^{-5}/P$
A	$5.06\times10^{-5}/P$	$2.87\times10^{-4}/P$	2.87×10^{-4}	$7.16\times10^{-5}/P$
CO_2	$3.18\times10^{-5}/P$	$1.80\times10^{-4}/P$	1.80×10^{-4}	$4.50\times10^{-5}/P$

and substituting for d from Equation (3-56) results in

$$V_r = \left(\frac{4S}{3x}\right)^2 \left(\frac{aV_{el}M}{m_e}\right) \left(\frac{1-K_3}{4a}\right)^2 \left[K_4 \ln\left(\frac{I_o^-}{I_{AN}^-}\right)\right]^2 . \qquad (3\text{-}58)$$

This states that the ion extraction potential is independent of the ion source design pressure, P_s, since d is caused to scale inversly with pressure.

In order to obtain good alignment of the electron beam over the ion exit aperture, and also to insure that the electron current density remain constant over the portion of the ionizing region from which the transmittable ions are extracted, it is a good practice to make the width of the beam somewhat wider than the diameter of the ion exit aperture. This can be accomplished by a scaling factor such that

$$K_5 = \frac{R}{w} . \qquad (3\text{-}59)$$

A value of K_5 less than 0.5 is necessary for the beam to cover the ion aperture. Combining these last three equations with Equations (3-31) and (3-54) to find the transmittable ion current in terms of the ion source pressure gives

$$I_T^+ = \left(\frac{16}{9} \times 10^{-6}\right)(K_5)\left(\frac{1-K_3}{4a}\right)^2 \left[K_4 \ln\left(\frac{I_o^-}{I_{AN}^-}\right)\right]^2 \left(\frac{K_2 S_p P_a}{48.4\times10^4 K_1}\right)^{1/2}$$

$$\left(\frac{aV_{el}M}{m_e}\right)\left(\frac{i_v S^3}{x^2}\right) P_s^{1/2} \qquad (3\text{-}60)$$

This equation states that with the use of scaling factors to define the geometrical relationships within the ionizing region of an ion source, and by holding the remaining parameters in this equation constant, then the maximum transmittable ion current increases with the square root of the maximum designed pressure limitation of the source. It is noted that several parameters do not appear in this equation. V_r, for example, has already been examined and found to be constant, independent of P_s. It is now necessary to examine the remaining parameters to determine if these are within the bounds of reasonableness as P_s is increased.

When the space potential of the ionizing plane changes within the ionizing region, a non-linearity will occur in the transmittable ion output current, due to a field curvature created between the ion extraction electrodes. This will change with the pressure as P_s is varied from zero up to the maximum designed pressure, P_s. It is therefore desirable to limit the degree of non-linearity which will occur over this range. When i_v is very small, this can be done by limiting the change of the value of α_2, such that $\Delta\alpha_2/\alpha_2$ corresponds to a marked degree of non-linearity (see curves plotted in Figure 3-3). Assuming i_v is very small, differentiating Equation (3-53) gives

$$\Delta\alpha_2 = aAi_v\Delta x \qquad (3\text{-}61)$$

However, the change in the value of x over a designed ion source pressure range is from x = 0 to x = x, or then $\Delta x = x$. Therefore, the non-linearity can be described by

$$\frac{\Delta\alpha_2}{\alpha_2} = \frac{Ai_v x}{1+Ai_v(x-1)} \qquad (3\text{-}62)$$

and thus

$$x = \frac{\left[\frac{1}{Ai_v} - 1\right]}{\left[\frac{\alpha_2}{\Delta\alpha_2} - 1\right]} \qquad (3\text{-}63)$$

From experimental data, the value of $\Delta a_2/a_2$ can be computed for a degree of non-linearity when i_v is small, and this can then be transposed into future design work.

The electron current density required to give the transmittable ion current as expressed by Equation (3-60) can then be found from Equation (3-51) as

$$J^- = \frac{i_v V_r \times 10^{-6}}{wt'}$$

However, the electron beam thickness, t', is a function of the ion energy spread as limited by the analyzer. This defines the thickness as

$$t' = \left(\frac{\Delta V_{ion}}{V_r}\right) d$$

and by substituting for V_r and d from Equations (3-56) and (3-58) gives

$$t' = (\Delta V_{ion}) \left(\frac{4S}{3x}\right)^{-2} \left(\frac{aV_{e1}M}{m_e}\right)^{-1} \left(\frac{1-K_3}{4a}\right)^{-1} \left[K_4 \ln\left(\frac{I_o^-}{I_{AN}^-}\right)\right]^{-1} P_s^{-1} \qquad (3\text{-}64)$$

The required electron current density to keep i_v constant as the maximum designed pressure varies can thus be written as

$$J^- = \left(\frac{i_v K_5}{\Delta V_{ion}}\right) (10^{-6}) \left(\frac{4S}{3x}\right)^4 \left(\frac{aV_{e1}M}{m_e}\right)^2 \left(\frac{1-K_3}{4a}\right)^3 \left[K_4 \ln\left(\frac{I_o^-}{I_{AN}^-}\right)\right]^3$$

$$\left(\frac{K_2 S_p P_a}{48.4 \times 10^4 K_1}\right)^{-1/2} P_s^{3/2} \qquad (3\text{-}65)$$

For an ion source designed to operate at higher pressures and retain a limited degree of non-linearity the dependence of the ion source parameters upon the maximum designed pressure can be abbreviated to the forms below:

$$R = C_1 \left(\frac{Q_a}{P_s}\right)^{1/2}$$

$$\ell_1 = \frac{C_2}{P_s}$$

$$V_r = C_3 P_s^{\,0}$$

$$J^- = C_4 Q_a^{-1/2} P_s^{3/2}$$

$$I_T^+ = C_5 (Q_a P_s)^{1/2}$$

This set of equations shows the dependence of the primary ion source parameters upon the two variables which define the system gas flow, i.e., the maximum ion source designed pressure, and the gas flow out of the analyzer. Here, the assumption is made that the conductance of the analyzer, C_a, is much greater than the speed of the pump, S_p. These equations are illustrated in Figure 3-4, and can then be interpreted as follows:

a. With the defined parameters of electron energy, gas species, ion energy spread, and electron transmission percentage to the anode, a set of dimensional relationships, or scaling factors can be generated relative to the ion exit aperture radius and the path length of the electron beam. These give the ionizing region dimensions as a function of the maximum ion source pressure, and the net gas flow out of the analyzer. It is then desirable to determine how the maximum transmittable ion current changes as the maximum ion source pressure is varied.

b. The maximum ion current output is governed by space charge limitations and non-linearity of the ion current as the pressure is changed. In certain specific ion sources where the non-linearity has been measured as a function of ion source pressure and electron current, the results can be placed in the context of Brubaker's source equations and the effective values of i_v and x determined. Thus, by maintaining these parameters constant, and the same relative dimensions, the maximum pressure can be varied without changing the degree of non-linearity of the source.

c. Since the relative parameters, x and i_v, are related through Equation (3-63) to a degree of non-linearity, $\Delta a_2/a_2$, when i_v is small, i_v must be held constant to maintain the same non-linearity as the pressure is varied. From Equation (3-51) it is seen that i_v would change as the ion source dimensions follow the change in the maximum pressure for V_r constant, if no other change were made. Thus, the electron current density must be adjusted to maintain the value of i_v.

d. As the maximum ion source pressure is increased, the result is (1) a shrinking of the ionizing region volume, (2) a decrease in the area of the electron entrance and ion exit apertures, and (3) an increase in the maximum transmittable ion current. The sensitivity of the source can then be expressed by

$$S = I_T^+ / P_S$$

$$\text{or} \quad S = C_5 Q_a^{1/2} P_s^{-1/2} \quad ,$$

which shows that while the transmittable ion current increases with the square root of the pressure from Equation (3-60), the ion source sensitivity will decrease with the square root of the maximum ion source pressure.

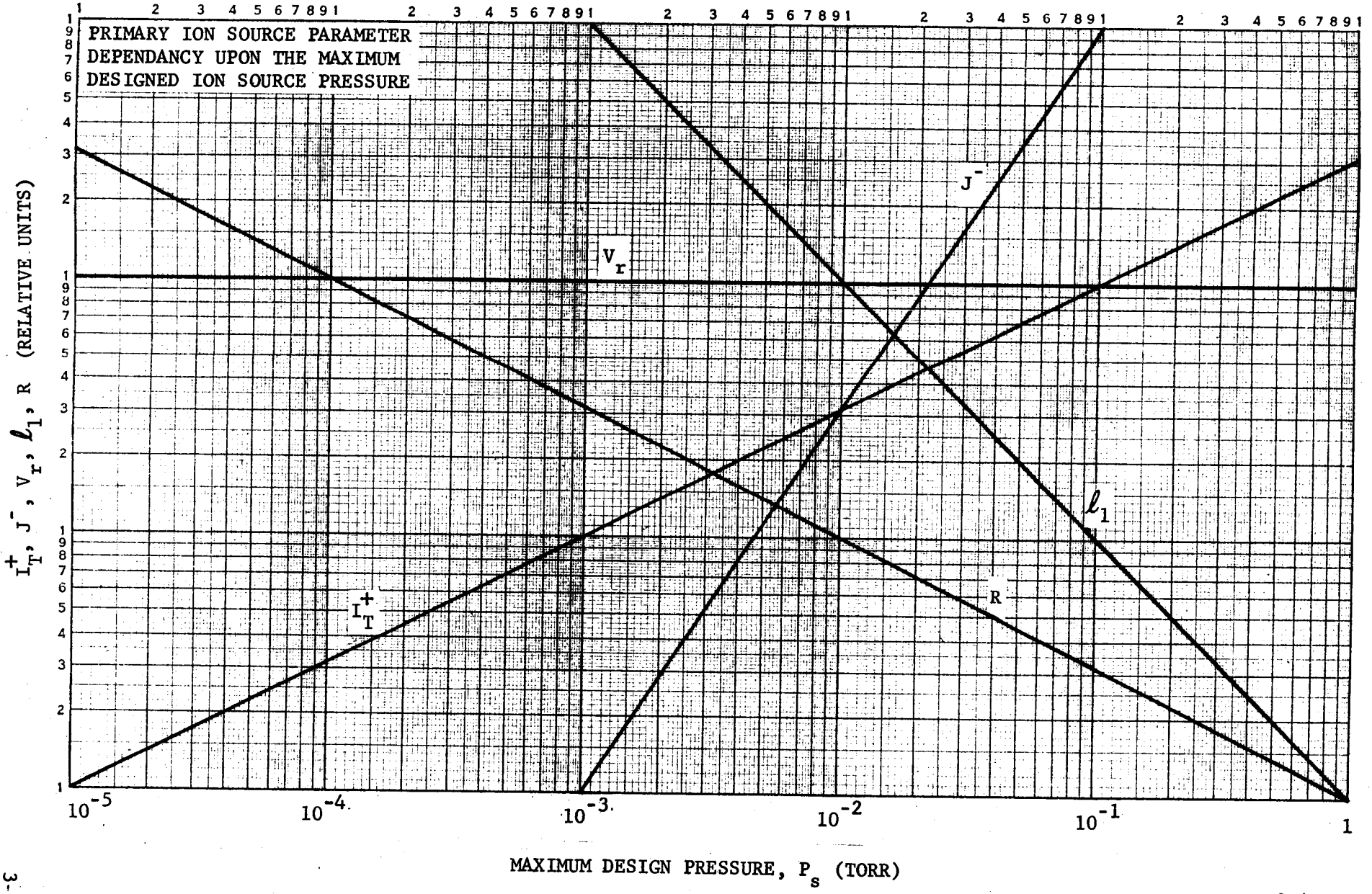
PRIMARY ION SOURCE PARAMETER
DEPENDANCY UPON THE MAXIMUM
DESIGNED ION SOURCE PRESSURE
I_T^+, J^-, V_r, ℓ_1, R (RELATIVE UNITS)
J^-
V_r
ℓ_1
R
I_T^+
10^{-5}
10^{-4}
10^{-3}
10^{-2}
10^{-1}
1
MAXIMUM DESIGN PRESSURE, P_s (TORR)

FIGURE 3-4

e. The gas flow, Q_a, regulated by the pumping system also governs the source conductance, and thus the value of R. Consequently, this "independent" control of the area for transmission allows for an increase in the ion current. This process of increasing the pumping capacity cannot, however, continue indefinitely, since eventually the ion exit aperture will exceed the maximum object size of the analyzer, or create too much field curvature within the ionizing region due to the large aperture size.

From the primary parameters derived above, the remaining ion source variables can be defined as a function of the maximum designed pressure.

The height of the electron entrance aperture, t, is found by substituting Equations (3-22) and (3-23) into the definition of K_1 which gives

$$\frac{R}{t} = 0.639 \frac{K_2}{K_5(K_1-1)} \left[\frac{t}{L_2}\right] K$$

However, since $\left[\frac{t}{L_2}\right] K$ will always remain constant for given L_2/t ratio, this equation reduces to the form

$$\frac{R}{t} = K_6 \tag{3-66}$$

where

$$K_6 = 0.639 \left[\frac{K_2}{K_5(K_1-1)}\right]\left[\frac{t}{L_2}\right] K$$

A magnetically aligned electron beam will have a thickness, t', within an orthogonal electric field which is defined by the expression

$$t' = t + \left(\frac{2m_e}{e}\right) \frac{V_r}{B_z^2 d} \tag{3-67}$$

Thus by substitution for the defined distances and the ion extraction potential, the required magnetic field strength to obtain a desired ion energy spread can be found. This is a function of the maximum pressure from the relationship

$$B_z = \left[\left(\frac{2m_e}{e}\right)\left(\frac{V_r}{d}\right)\left(\frac{1}{t'-t}\right)\right]^{1/2} . \tag{3-68}$$

A region containing perpendicular magnetic and electric fields will "bend" an electron beam traveling along the magnetic field lines orthogonally to the two crossed fields. The effective angle through which it is "bent" can be expressed by

$$\theta = \tan^{-1}\left(\frac{V_r}{B_z v_e d}\right) . \tag{3-69}$$

θ can be found as a function of the maximum pressure by substitution for the ion extraction potential, the magnetic field, and the distance between the ion extraction electrodes.

3.2.3 PHYSICAL LIMITATIONS

While the equations developed in the previous sections are theoretically valid for the design of a high pressure ion source, physical limitations will prevent them from being realized due to the following characteristics:

a. The apertures which are controlling the gas flow will approach the limit of machinability unless the pumping speed is increased. This cannot be increased indefinitely however due to the reasons previously explained.

b. The electron current density cannot be increased beyond the limit of what can be obtained by focusing electrons from the filament to the aperture. Consequently, when the emission density reaches a maximum, the constant i_v will not be maintained to give a defined non-linearity unless the ion extraction potential is changed. This will change the value of the transmittable ion current.

c. There exists a maximum current, ion or electron, which can be transmitted through an aperture due to space charge.

d. With the distance, d, decreasing between the repeller and accelerator as the pressure is increased, and with V_r remaining constant, the distance will reduce to the point where voltage breakdown can occur.

It was previously seen that to keep the relative parameter, i_v, constant, it is necessary to maintain a constant electron current, $\bar{J}wt'$, to the anode. However, since w is scaling with R, and t' is a function of d, then the electron current density must increase with the 3/2 power of the maximum pressure to maintain the value of i_v. Now, if the electron current density reaches a maximum value, J_{max}, due to physical limitations of the emission system, then to maintain the value of i_v, the ion extraction potential can be changed with pressure. Thus in the limiting case, this potential can be expressed as

$$V_r = \left[\frac{[\Delta V_{ion}]\,[\bar{J}_{max}]\,[10^6]}{K_5\, i_v}\right]^{1/2} \left(\frac{K_2 S_p P_a}{48.4 \times 10^4 K_1}\right)^{1/4} \left(\frac{1-K_3}{4a}\right)^{1/2} \left[K_4 \ln\left(\frac{\bar{I}_o}{\bar{I}_{AN}}\right)\right]^{1/2} P_s^{-3/4} \quad . \tag{3-70}$$

The transmittable ion current in the case where the electron current density has reached a maximum then becomes

$$I_T^+ = \left(\frac{3\pi}{4}\right)\left[\left[\Delta V_{ion}\right]\left[J_{max}^-\right]\right]^{3/4}\left[xi_v^{1/4}\ K_5^{1/4}\right]\ (10^{-6})^{1/4}\left(\frac{m_e}{aV_{el}M}\right)^{1/2}$$

$$\left(\frac{K_2 S_p P_a}{48.4 \times 10^4 K_1}\right)^{7/8}\left(\frac{1-K_3}{4a}\right)^{-1/4}\left[K_4 \ln\left(\frac{I_o^-}{I_{AN}^-}\right)\right]^{-1/4} P_s^{-5/8} \qquad (3\text{-}71)$$

From Equation (3-70), substitution for V_r into Equations (3-68) and (3-69) will then give the values of the magnetic field, B_z, and the electron beam walking angle, θ, as a function of the maximum pressure when the electron current density becomes limited.

Space charge will limit the amount of electron or ion current which can be transmitted through a tunnel aperture. Spangenberg[4] gives the relationship for the maximum ion current transmittable through a circular aperture as

$$I_{SC}^+\Big|_{\substack{TUN\\MAX}} = 0.550 \times 10^{-4}\ V_r^{3/2}\left[\frac{R}{L_1}\right]^2\left[\frac{m_e}{M}\right]^{1/2} . \qquad (3\text{-}72)$$

Thus, the maximum ion current due to space charge in the aperture is a function of the ion extraction potential if the R/L_1 ratio remains constant as defined for the constant K_2. It is then seen that up to the point where the electron current density becomes limited, this maximum current will remain constant as the maximum pressure is varied, and beyond this point, it will change inversely proportional to the 9/8 power of the pressure.

Spangenberg[4] also gives the relationship for the space charge limiting of a magnetically confined electron beam passing through a tunnel aperture. In this case, beam spreading does not occur, so that the space charge limit is only created by an increase in the current density. This happens when the potential of the center of the electron beam drops to the potential of the source. For a beam which completely fills the aperture, the limit then occurs when

$$I_{SC}^-\Big|_{\substack{TUN\\MAX}} = 1.025\left[(V_{el})_{APERTURE} \times 10^{-3}\right]^{3/2} \qquad (3\text{-}73)$$

This expression shows that the space charge limit of a magnetically confined electron beam passing through a tunnel aperture is independent of the dimensions of the aperture, and solely dependent upon the energy of the electrons upon reaching the aperture. Alternatively, J^- can be increased up to the limit of the emission system by increasing the energy of the electrons before they pass through

the aperture. The minimum energy thus required of the electrons to pass the necessary current density to the ionizing region is found to be

$$V_{el}\Big|_{\substack{\text{APERTURE}\\\text{MINIMUM}}} = (9.833 \times 10^{-2})\,(i_v)^{2/3}\left(\frac{4S}{3x}\right)^{4/3}\left(\frac{aV_{el}M}{m_e}\right)^{2/3}\left(\frac{1-K_3}{4a}\right)^{4/3}\left[K_4 \ln\left(\frac{I_o^-}{I_{AN}^-}\right)\right]^{4/3}, \tag{3-74}$$

up to the limit of the emission system. Beyond this limit, this expression then changes to

$$V_{el}\Big|_{\substack{\text{APERTURE}\\\text{MINIMUM}}} = (9.833)\left[\frac{(\Delta V_{ion})\,(J_{max}^-)\,(i_v)}{K_5}\right]^{1/3}\left(\frac{K_2 S_p P_a}{48.4 \times 10^4 K_1}\right)^{1/6}\left(\frac{1-K_3}{4a}\right)^{1/3}\left[K_4 \ln\left(\frac{I_o^-}{I_{AN}^-}\right)\right]^{1/3} P_s^{-1/2}. \tag{3-75}$$

The last physical limitation involves the approach toward breakdown due to the decreasing repeller-accelerator distance, d, while the maximum pressure is increasing and the extraction potential is remaining constant. A plot of voltage breakdown versus the pressure times the electrode spacing is given in Figure 3-5. However, the abscissa of the curve, $P_s \times d$, is a constant, since substitution for the distance gives

$$P_s \times d = \left(\frac{1-K_3}{4a}\right)\left[K_4 \ln\left(\frac{I_o^-}{I_{AN}^-}\right)\right] \tag{3-76}$$

and thus the breakdown voltage will remain constant as the maximum designed pressure is varied. The curve shown in Figure 3-5 represents the idealized case, where no sharp corners exist, and no charged particles are present within the spacing. In an ion source, this is not the case, and the effects from these additional conditions are not known, so that the degree of confidence in the allowable voltage levels is rather limited.

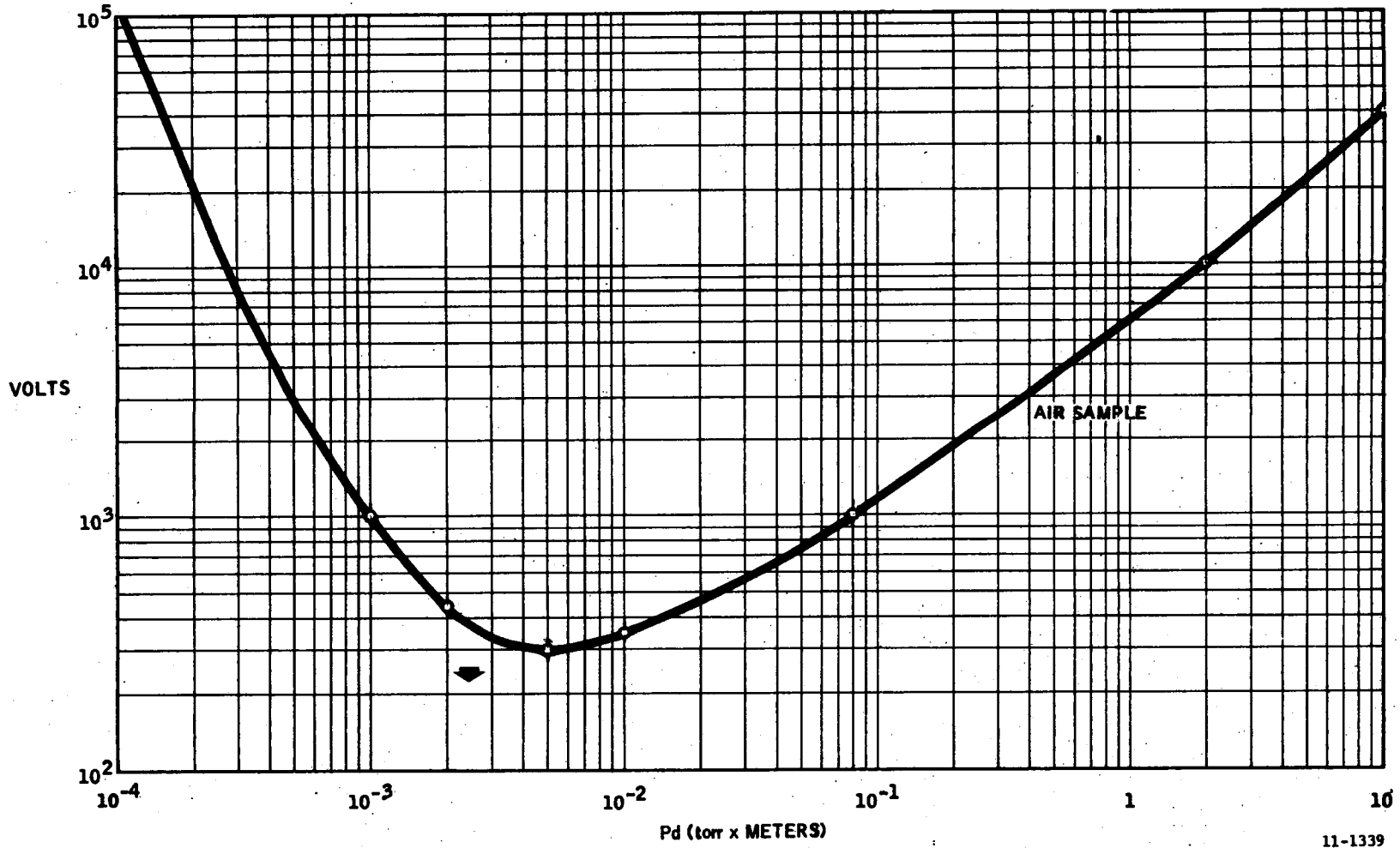

P = PRESSURE (torr)

d = ELECTRODE SPACING (METERS)

FIGURE 3-5

3.3 ION SOURCE MASS DISCRIMINATION

An ion source utilizing a magnetic field to align and constrain the ionizing electron beam will also create mass discriminating deflections of the ions generated in the same manner as a magnetic analyzer section of a mass spectrometer. The deflections will thus be dependent upon the molecular mass-to-charge ratio.

While it is possible to derive expressions for these deflections, the derivations are dependent upon (1) a knowledge of the magnetic field, (2) the flux density versus distance along the ion source axis from the point of ionization, and (3) the ion energy with respect to the distance traveled.

Thus, it appears more reasonable to analyze the mass discrimination by utilizing a split ion focusing lens in the design of the test model and measure these deflections by observing the spread potential required to focus the different masses out of the source.

3.4 SYSTEM TIME RESPONSE ANALYSIS

As derived in Section 3.1.1, the ion source and analyzer pressure changes as a function of time with the use of a pump can be expressed by

$$\frac{dP_s}{dt} = \frac{1}{V_s}\left[P_o C_o - (C_o + C_s)\, P_s + P_a C_s\right] \tag{3-6}$$

and

$$\frac{dP_a}{dt} = \frac{1}{V_a}\left[P_s C_s - \left(C_s + \frac{C_a S_p}{S_p + C_a}\right) P_a\right] \tag{3-7}$$

Converting these two equations to their respective LaPlace transforms gives

$$sP_s(s) - P_s(o) = \frac{1}{V_s}\left[C_o P_o(s) - (C_o + C_s)\, P_s(s) + C_s P_a(s)\right] \tag{3-77}$$

and

$$sP_a(s) - P_a(o) = \frac{1}{V_a}\left[C_s P_s(s) - \left(C_s + \frac{C_a S_p}{S_p + C_a}\right) P_a(s)\right] \tag{3-78}$$

These simultaneous equations have been solved for a step function response, and after taking the inverse transform have the form

$$P_s(t) = A_1 u(t) + B_1 e^{-n_1 t} + C_1 e^{-n_2 t} \tag{3-79}$$

and

$$P_a(t) = A_2 u(t) + B_2 e^{-n_3 t} + C_2 e^{-n_1 t} + D e^{-n_2 t} \tag{3-80}$$

In order to analyze these responses for variations of any or all of the system parameters, a computer program was generated for these solutions as shown in Appendix A.

Similarly, the expressions developed in Section 3.1.2 for the system response without a pump were evaluated and computerized for a step function change in the external pressure. This program is listed in Appendix B. The results of the Time Response analysis are discussed in Section 5.2.

4. SOLUTION TO THE TASK REQUIREMENT

4.1 DIMENSIONAL CONSIDERATIONS

The system for testing the ion source consisted of a quadrupole mass spectrometer with an attached pumping system of one litter/sec. In order to protect the filament and electron gun, it was necessary to utilize differential pumping and to limit the maximum analyzer pressure to 1×10^{-5} torr. For a maximum ion source pressure of 1×10^{-2} torr the differential pumping ratio was thus, 1×10^{3}. Assuming the conductance of the analyzer to be much greater than the speed of the pump, from Equation (3-9), the gas flow rate of the analyzer, Q_a, is limited to 1×10^{-5} torr-liters/second. The ion source gas conductance is found to be one cc/second. The gas flow is then divided through the electron entrance and ion exit apertures which together must give the desired total gas conductance. The radius of the ion exit aperture becomes, from Equation (3-31) and for the above values;

$$R = 4.55 \times 10^{-5} \left[\frac{K_2}{K_1}\right]^{1/2} \quad \text{(meters)}, \qquad (4\text{-}1)$$

where K_2 and K_1 are the arbitrary scaling constants as defined in Section 3.1.6.

The critical dimensions of the ionizing region, ℓ_1 and ℓ_2, are related to P_s by the equations developed in Section 3.2.1. For an air sample at 1×10^{-2} torr, the values of the ion path length, ℓ_2, are tabulated in Table 4-1 versus I^+/I_o^+

TABLE 4-1

$P_s = 1 \times 10^{-2}$ torr — Air Sample

I^+/I_o^+	ℓ_2 (meters)	ℓ_2 (inches)
99%	6.85×10^{-5}	0.00270
98%	1.36×10^{-4}	0.00536
95%	3.51×10^{-4}	0.0138

From Equation (3-46), and Table 4-1, the length of the electron beam path is then found for a chosen I^+/I_o^+ transmission percentage. However, regulation of the anode current will increase I_o^-. This in turn will increase I_o^+ such that the I^+ output will remain linear with the sample pressure in the source. To first order, this correction will continue up to the limiting emission density of the filament.

For practical reasons of tolerances and aperture sizes, the 0.0138 inch value for ℓ_2 was chosen. An 0.028 inch spacing between the repeller and accelerator is required for an electron beam equally spaced between these two electrodes. This value provides 99% transmission of the ions at 1.95×10^{-3} torr, 98% at 3.88×10^{-3} torr and 95% at 10^{-2} torr. Anode current compensation is expected to reduce the net non-linearity to below 2%. Thus, the electron current path length, ℓ_1, is found from Equation (3-46) to be

$$\ell_1 = \frac{4\ell_2}{(1-K_3)} = \frac{1.404 \times 10^{-4}}{(1-K_3)} \quad \text{(meters)} \tag{4-2}$$

The ion extraction electrode distance, d, can then be defined from Equation (3-56) by

$$d = \frac{\ell_2}{a} = \frac{3.51 \times 10^{-4}}{a} \quad \text{(meters)} \tag{4-3}$$

where K_4 is chosen for an air sample, and a is the fractional location of the electron beam. By placing the center of the electron beam in the middle of the extraction electrodes, the constant, a, becomes o.5, and thus $d = 7.01 \times 10^{-4}$ meters. This is done to try to insure that all of the electron current within the ionizing region will only strike the anode surface and not any of the other electrodes.

The electron beam width is expressed by Equation (3-59), such that

$$w = \frac{R}{K_5} = \frac{4.55 \times 10^{-5}}{K_5} \left[\frac{K_2}{K_1}\right]^{1/2} \quad \text{(meters)} \tag{4-4}$$

This width is therefore only dependent upon arbitrary scaling constants to be chosen. Consequently, since the beam width is set equal to the electron entrance slit width, the aperture height can then be derived from Equation (3-66). This gives

$$t = \frac{R}{K_6} = \frac{4.55 \times 10^{-5}}{K_6} \left[\frac{K_2}{K_1}\right]^{1/2} \quad \text{(meters)} \tag{4-5}$$

Here, K_6 is defined by Equation (3-66).

The arbitrary constants involved were chosen on the basis of the following discussion:

a. The gas conductance out of the source was arbitrarily set such that equal conductances would be obtained through both the electron entrance and ion exit apertures. Thus, from Equation (3-25), $K_1 = 2$.

b. Since the transmittable ion current is dependent upon the square of the radius of the ion exit aperture as shown in Equation (3-48), it is then desirable to enlarge the diameter of this hole. Thus, if the diameter is increased, then the length of the aperture must increase at a much faster rate to keep the conductance constant. As this length increases however, the exiting ions will be affected by the fringe fields existing from the gradients of the ion lens system and the ionizing region at each end of the aperture. Thus, to compromise the above effects, a length to diameter ratio of 2 was chosen for the ion exit aperture which, from Equation (3-29), sets $K_2 = 3.72$.

c. The position of the ion exit aperture is best located in the center of the ionizing region in order to reduce the effects of field distortion around the perimeter of the extraction field. A more uniform field and defined electron energy thus results. The position of the aperture at this point is nominally one half of the electron beam path length, ℓ_1, and thus $K_3 = 0.5$.

d. To obtain alignment of the ionizing electron beam above the ion exit aperture, and to avoid misalignments caused by variations in the extraction potential, V_r, which can displace the beam sideways in the EXB field, it is desirable to make the electron beam width wider than the ion exit aperture diameter. A value of four times the diameter of the aperture was chosen. This allows the beam to be 1-1/2 times this diameter on each side of the aperture. From Equation (3-59), $K_5 = 0.125$.

e. The height of the electron entrance aperture, t, is determined from the constant K_6 as defined in Equation (3-66), and the ion exit aperture radius, R. But this value is also dependent upon the height to length ratio, t/L_2, which is an arbitrary choice. A compromise was then based upon practical considerations of machinability and providing the correct conductance. To allow for these considerations, an aperture height of 0.003 in. was chosen which gives the required conductance for the aperture when the length, L_2, is 0.063 in. The calculated value for K_6 is thus 1.032.

The values of the critical dimensions for the ion source using these constants are tabulated below in Table 4-2.

TABLE 4-2

R	$= 6.21 \times 10^{-5}$	meters	$(2.45 \times 10^{-3}$ inches)
ℓ_2	$= 3.51 \times 10^{-4}$	meters	$(1.38 \times 10^{-3}$ inches)
ℓ_1	$= 2.81 \times 10^{-3}$	meters	$(1.11 \times 10^{-2}$ inches)
d	$= 7.01 \times 10^{-4}$	meters	$(2.76 \times 10^{-2}$ inches)
w	$= 4.97 \times 10^{-4}$	meters	$(1.96 \times 10^{-2}$ inches)
t	$= 7.62 \times 10^{-5}$	meters	$(3.00 \times 10^{-3}$ inches)
L_1	$= 2.48 \times 10^{-4}$	meters	$(9.75 \times 10^{-3}$ inches)
L_2	$= 1.60 \times 10^{-3}$	meters	$(6.30 \times 10^{-2}$ inches)

4.2 ACTIVE DESIGN FACTORS

The active design factors are the ionizing electron current density, the ion extraction potential, and electron beam energy in the ionizing region. These interrelated parameters are the variables which must be adapted to both the dimensions and each other, in order to realize the design goals.

From Equation (3-57), substitution for the designed pressure, the extraction electrode distance, d, the constant, a, the electron mass, and assuming the ion mass for nitrogen as the design-center mass, then the ion extraction potential can be expressed by

$$V_r = 2.23 \times 10^{-6} \left(\frac{S^2 V_{el}}{x^2} \right) \tag{4-6}$$

From Equation (3-51), it is seen that the electron current density is dependent upon the ion extraction potential, the width and thickness of the electron beam, and the space charge parameter, i_v. However, the thickness of the electron beam is seen from Equation (3-64) to be dependent upon the fixed ion energy spread acceptable by the analyzer. For the present application, the quadrupole mass filter was designed to accept ions having an energy spread of up to 15 volts. But, to allow for variations in the magnetic field strength which would change the thickness of the beam for a given gradient within the ionizing region, a value for ΔV_{ion} of 10 volts is assumed. Thus, the electron current density can be found to be:

$$J^- = 1.427 \times 10^{-12} \left(\frac{i_v S^4 V_{el}^2}{x^4} \right) . \tag{4-7}$$

Solving this expression for $(S^2 V_{e1}/x^2)$, and substituting in Equation (4-6), gives,

$$V_r = 1.865 \left[\frac{J^-}{w}\right]^{1/2} \quad . \tag{4-8}$$

It is important at this point to know what emission densities can be obtained from the filament sources available. A previously designed non-magnetic ion source has given electron emission densities of 90 amps/meter^2 through an aperture 0.010 inch high by 0.060 inch wide, for total filament emissions of between 100 and 120 micro-amperes. However, with a magnetically aligned electron beam, higher emission densities can be obtained, due to improved confinement of the beam. Using the proven density, the ion extraction potential is thus

$$V_r = \frac{17.75}{(i_v)^{1/2}} \tag{4-9}$$

The relative parameter, i_v, is best chosen to a small value in order that the change in the spatial potential, $\Delta a_2/a_2$, is small as x changes from x = o to $x = x_1$. However, it is also desirable that V_r not become too large. Thus, a value was chosen of $i_v = 0.20$ such that

$$V_r = 39.7 \text{ volts} \quad . \tag{4-10}$$

Substituting this value into Equation (4-6), then it is seen that

$$\frac{V_{e1} S^2}{x^2} = 1.780 \times 10^7 \quad . \tag{4-11}$$

For the value of i_v chosen above, the value of x at the maximum designed pressure will then determine the non-linearity, which will be created due to the changing potential at the ionizing plane. On one type of mass spectrometer,[5] having a similar geometry in the ion source, a 3 percent interference (non-linearity) occurred when $\Delta a_2/a_2 = 0.0233$. However, it is felt that the design value of $\Delta a_2/a_2$ should be more conservative. For this reason, a value of $x = \sqrt{2}$ was used to evaluate the parameter $V_{e1}S^2$. Thus, Equation (4-11) becomes

$$V_{e1} S^2 = 3.56 \times 10^{-7} \quad . \tag{4-12}$$

The ionization crossection, S, is dependent upon the ionizing electron energy, and has been thoroughly studied for many gas species. Between 40 and 100 volts of electron energy, the cross sections for nitrogen and oxygen are nearly identical, so that for a nitrogen sample, the dependence of S upon V_{e1} is tabulated in Table 4-3.

TABLE 4-3

V_{e1} (volts)	S (AMP $(I^+_{N_2})$/AMP (I^-)-meter-torr)
40	600
50	800
60	900
70	950
80	980
90	1010
100	1050

From this table, the values of $V_{e1}S^2$ for nitrogen have been computed, and are plotted as a function of the ionizing electron energy, V_{e1}, in Figure 4-1. From this curve, it is seen that to satisfy Equation (4-12), the ionizing electron energy must be

$$V_{e1} = 52 \text{ volts} \tag{4-13}$$

With this value determined, it is then possible to calculate the depression in the spacial potential of the ionizing plane when the maximum pressure of 1×10^{-2} torr is reached in the ion source. From Equation (3-62), it is seen that

$$\frac{\Delta a_2}{a_2} = 0.00526 \tag{4-14}$$

which is considerably lower than the value which gave a 3 percent non-linearity with the cycloidal focusing mass spectrometer.

The required electron current in the ionizing region, without collisional effects, can thus be derived from the relationships

$$I^- = J^- wt' \text{ or } I^- = i_v V_r \quad . \tag{4-15}$$

Substitution of these determined values gives

$$I^- = 7.94 \times 10^{-6} \text{ amperes} \quad . \tag{4-16}$$

With the constraints of the problem and the values chosen, the ion source appears to be capable of operation to 1×10^{-2} torr.

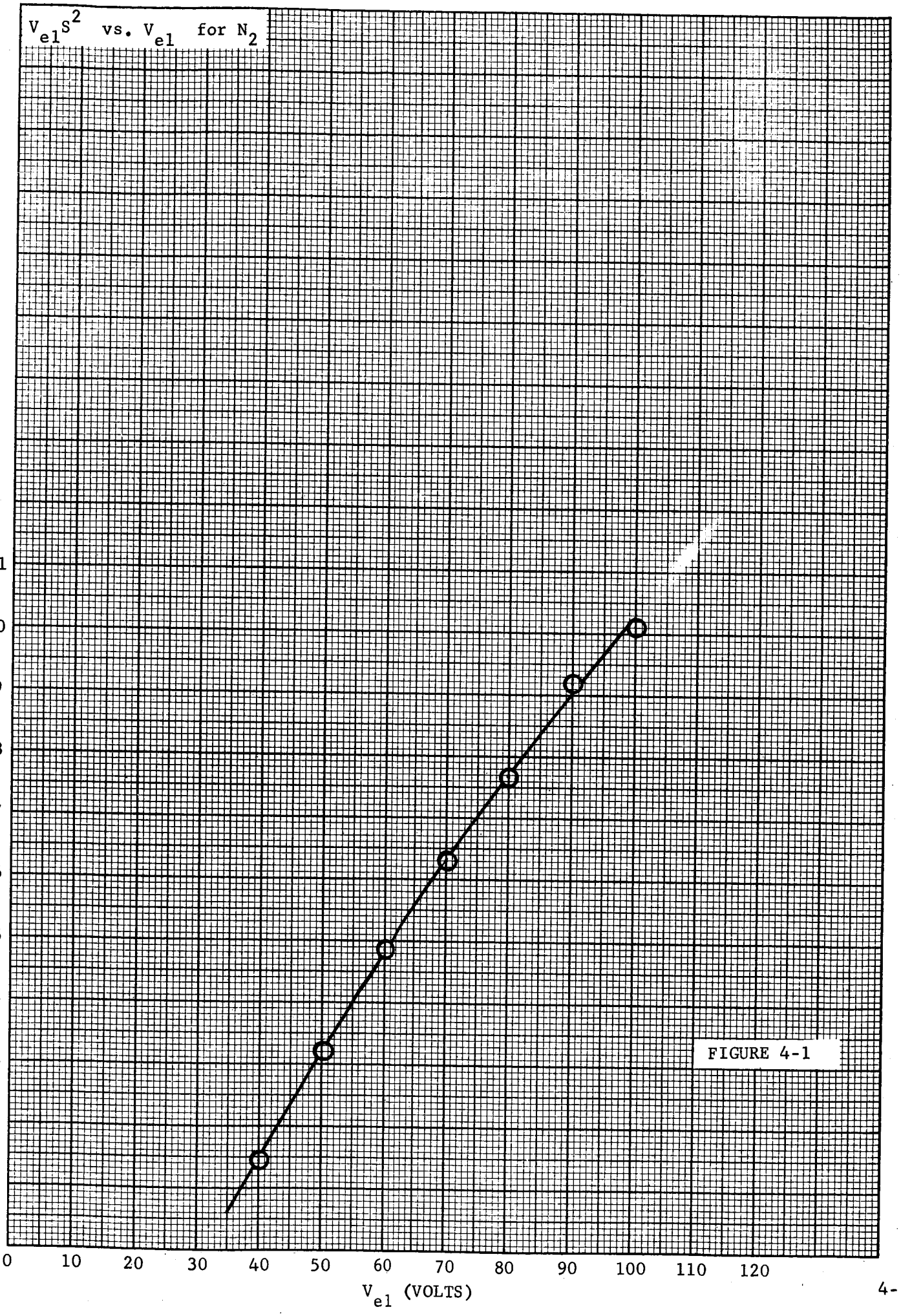
$V_{el}S^2$ vs. V_{el} for N_2
$V_{el}S^2$ (x 10^7)
11
10
9
8
7
6
5
4
3
2
1
0
10
20
30
40
50
60
70
80
90
100
110
120
V_{el} (VOLTS)

FIGURE 4-1

The transmittable ion current for the parameters derived can then be found from Equation (3-60), which for a nitrogen sample at 1×10^{-2} torr gives

$$I_T^+ = 1.608 \times 10^{-9} \text{ amperes} \tag{4-17}$$

However, this current corresponds to the maximum transmission of ion current from the first aperture. Due to the optics and apertures of the remainder of the ion focusing system, it is assumed that the output current of the ion source into the quadrupole analyzer will only be 10 percent of the transmittable ion current from the first aperture. This ion transmission percentage agrees approximately with transmission data taken on previously designed ion sources. Consequently, the final ion output current of the source at 1×10^{-2} torr of nitrogen should be

$$I_{N_2}^+ \Big|_{\text{OUTPUT}} \approx 1.6 \times 10^{-10} \text{ amperes} \quad . \tag{4-18}$$

Thus, the ion source sensitivity will be

$$\text{SENSITIVITY} \Big|_{N_2} \approx 1.6 \times 10^{-8} \text{ amps/torr} \tag{4-19}$$

which satisfies the design goals as stated in Section 2.0.

4.3 PASSIVE DESIGN FACTORS

The passive design factors of the ion source consist of the design parameters which are dependent upon the values of the active design factors determined in Section 4.2. These include the resultant thickness of the electron beam, t', the required magnetic field to produce this thickness, B_z, the walking angle of the electron beam, θ, and the physical limitations placed upon the active design factors.

The thickness of the electron beam is a defined parameter which is a function of the ion energy spread, ΔV_{ion}, acceptable by the analyzer. As stated in Section 4.2, the source is to be designed to give an energy spread of 10 volts, so that from Equation (3-64), the required thickness is

$$t' = 1.768 \times 10^{-4} \text{ meters} \tag{4-20}$$

Substituting this value into Equation (3-68), the required magnetic field, B_z, can be found, which gives

$$\begin{aligned} B_z &= 8.006 \times 10^{-2} \text{ webers/meter}^2 \\ &\approx 800 \text{ gauss} \end{aligned} \tag{4-21}$$

The walking angle, θ, of the electron beam can thus be calculated from Equation (3-69) which gives the result that

$$\theta = 9.38^{\circ} \tag{4-22}$$

Since the designed parameters do not imply a limitation occurring due to emission limiting of the filament, the physical limitations implied by Equations (3-70) and (3-71) will not be present in the design being considered. It is then necessary to examine the space-charge limiting which will occur in the tunnel apertures to see if the designed currents will pass through the apertures. The maximum current which can be passed through the ion exit aperture is defined by the relationship of the parameters expressed by Equation (3-72). Substituting the values previously derived, it is then seen that

$$I_{SC}^{+}\Big|_{\substack{TUN \\ MAX}} = 3.81 \times 10^{-6} \text{ amperes} \tag{4-23}$$

which is much greater than the maximum ion current transmittable at the maximum pressure defined by Equation (4-18).

For the electron entrance aperture, Equation (3-73) defines the space charge limit for the electron current. Assuming that the potential of the electron entrance aperture is the same as the ion accelerator in which the ion exit aperture is located, it can be written that

$$V_{el} = V_{el}\Big|_{APERTURE} + \frac{1}{2} V_r \tag{4-24}$$

Rearranging terms and substituting values gives

$$V_{el}\Big|_{APERTURE} = 32 \text{ volts} \tag{4-25}$$

The maximum current passable through the electron entrance aperture is thus

$$I_{SC}^{-}\Big|_{\substack{TUN \\ MAX}} = 5.92 \times 10^{-3} \text{ amperes} \tag{4-26}$$

which is much greater than the required electron current, and moreover much greater than can be supplied by the emission system.

These calculations show that the effects of space charge in the tunnel apertures will be negligible.

The breakdown potential for a designed maximum pressure of 1×10^{-2} torr can be found from the curve illustrated in Figure 3-5. For the design values, $P_S xd = 7.01 \times 10^{-6}$ torr-meters which would have a breakdown voltage of greater than 10^5 volts without the presence of charged particles or sharp corners within the ionizing region. The 40 volt extraction potential is also below the minimum value of 300 volts for pure gaseous breakdown.

5. DESIGN OF THE TEST MODEL

The design of a high pressure ion source capable of operating at pressures up to 1×10^{-2} torr was accomplished with a goal of utilizing the instrument with a previously designed quadrupole mass spectrometer. The dimensions above were utilized to define the spacings of the ion source for compatible operation at the maximum operating pressure. Further analysis and design was required, however, to determine the size of the magnet to obtain the necessary B_z field, and to compute the time response of the designed system. The final configuration of the ion source assembly is illustrated in Figure 5-1. An exploded view of the ionizing region cross section is shown in Figure 5-2, with the various electrodes being called out.

5.1 MAGNET DESIGN

Due to the relatively low magnetic field required, and the limited spacing in the source region, the use of Placovar [6] was incorporated for the magnet material. While expensive, this material has distinct advantages for space-constricted designs since it has a very high energy product.

Figures 5-3 and 5-4 show the demagnitization curve and effect of high temperatures, respectively, upon the Placovar material. The flux curve versus temperature is for the initial exposure of the material to a desired temperature, and subsequent exposures to temperatures equal to or lower than the initial one do not reduce the flux level further. Thus, to obtain a B_z field of at least 800 gauss as derived in Equation (4-21) and a bakeout capability of 350°C, then from Figure 5-4, the magnet must be chargeable to at least 915 gauss in the gap. To allow for a safety factor in the approach, the magnet flux density obtainable in the gap was chosen at 1000 gauss.

Due to the relative sizes of the ion source material to be placed between the magnet poles, the length of the magnet gap was defined in the design to be approximately 0.600 inch. Furthermore, for the ion source to fit within the housing, the length of the pole face material on each side of the source was restricted to about 0.300 inch.

To obtain the lowest leakage factor of the magnet, the optimum magnet-yoke combination configuration is a construction where the magnet material is located at the pole faces with the connecting yoke made from high parmeability soft iron. This is illustrated in Figure 5-5.

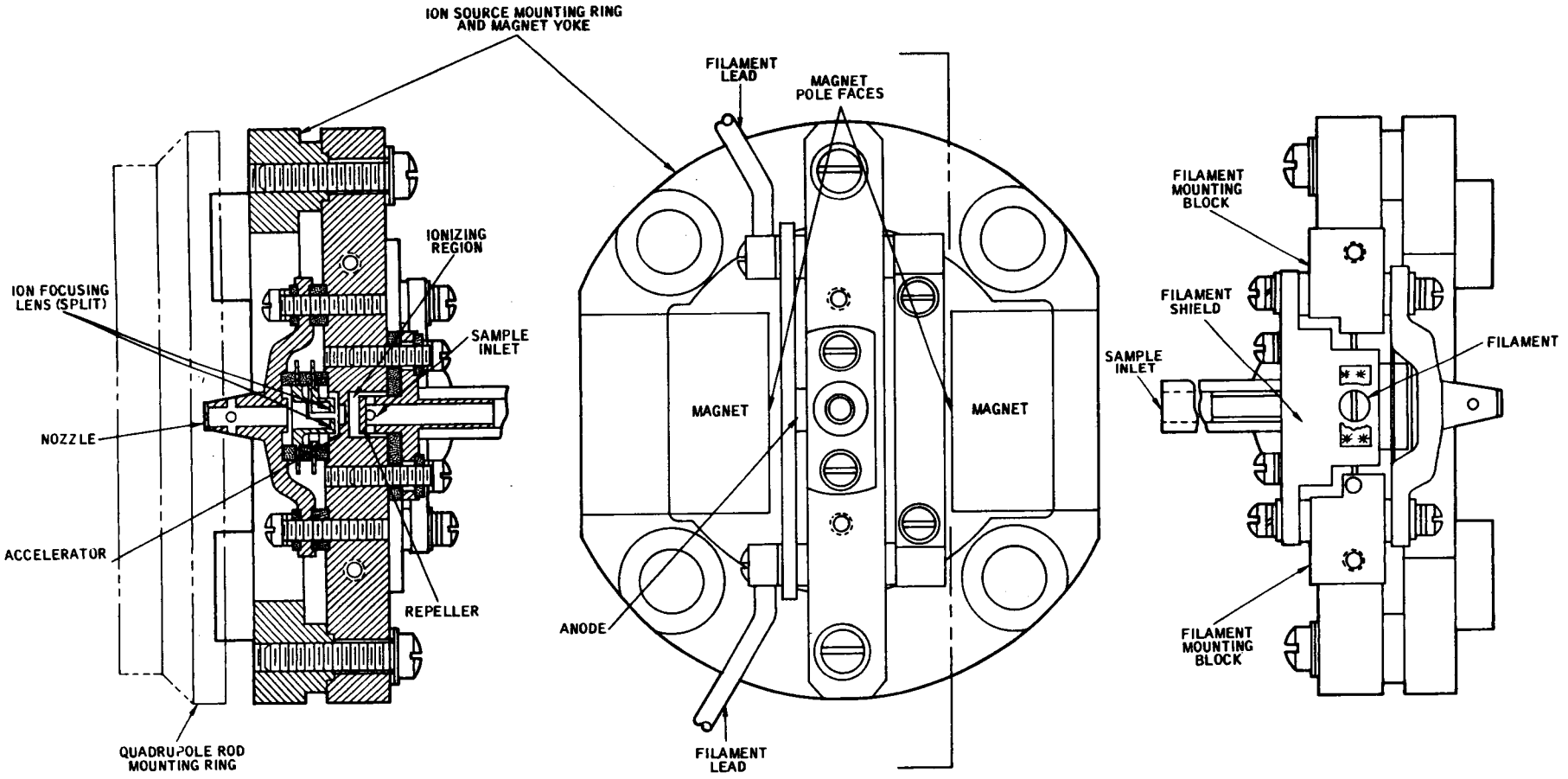

FIGURE 5-1 ION SOURCE ASSEMBLY

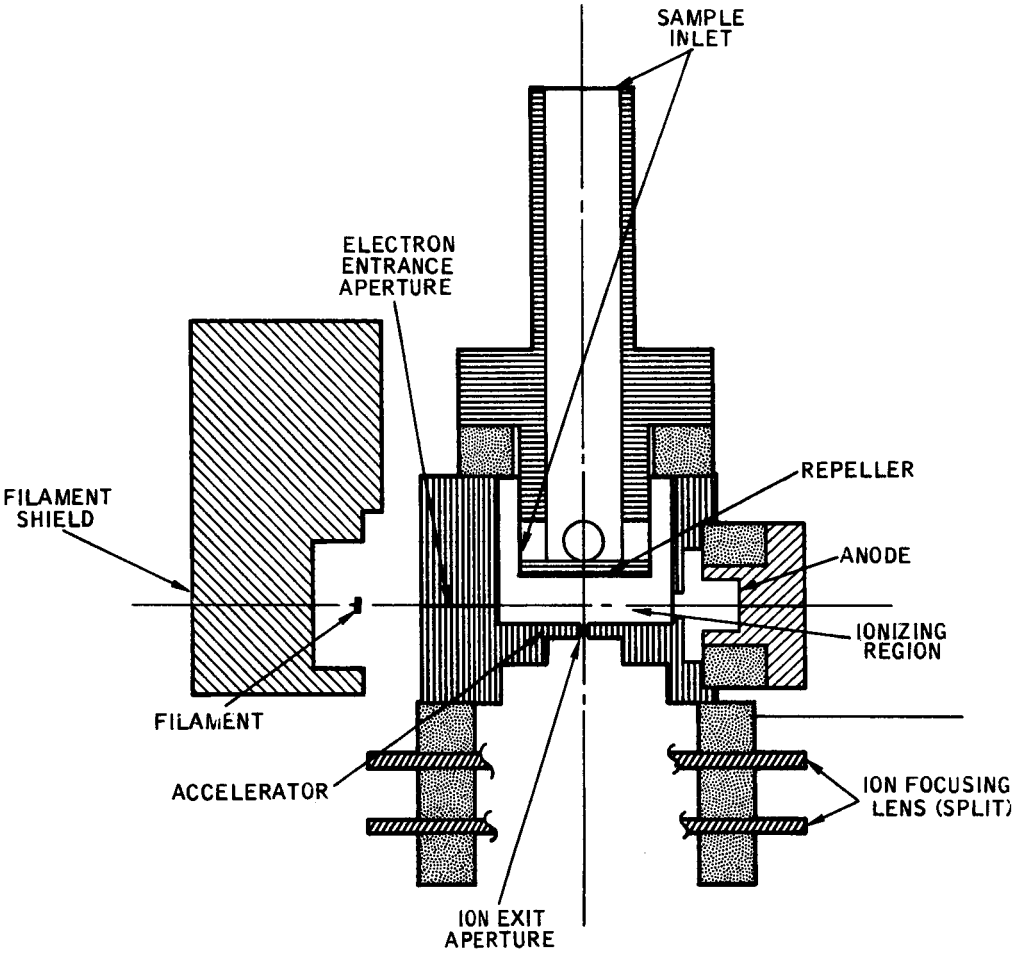

FIGURE 5-2
IONIZING REGION CROSS SECTION

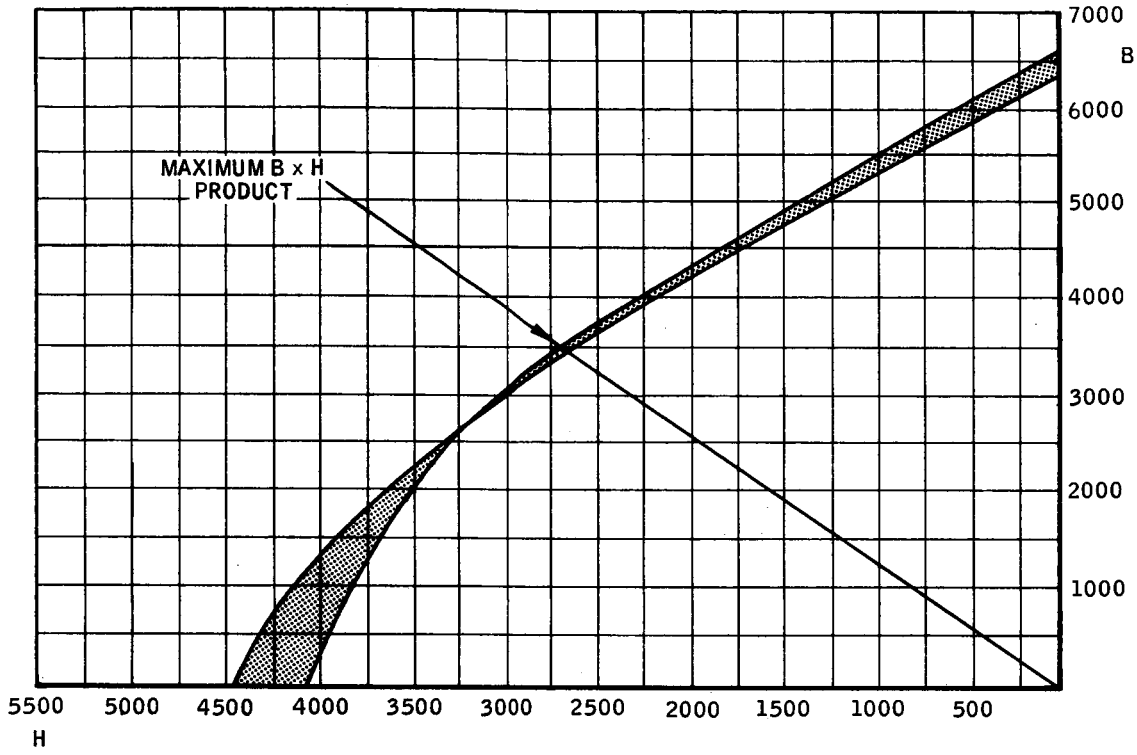

FIGURE 5-3

B VS H DEMAGNETIZATION CURVES ON PLACOVAR DEPENDANT ON HEAT TREATMENT

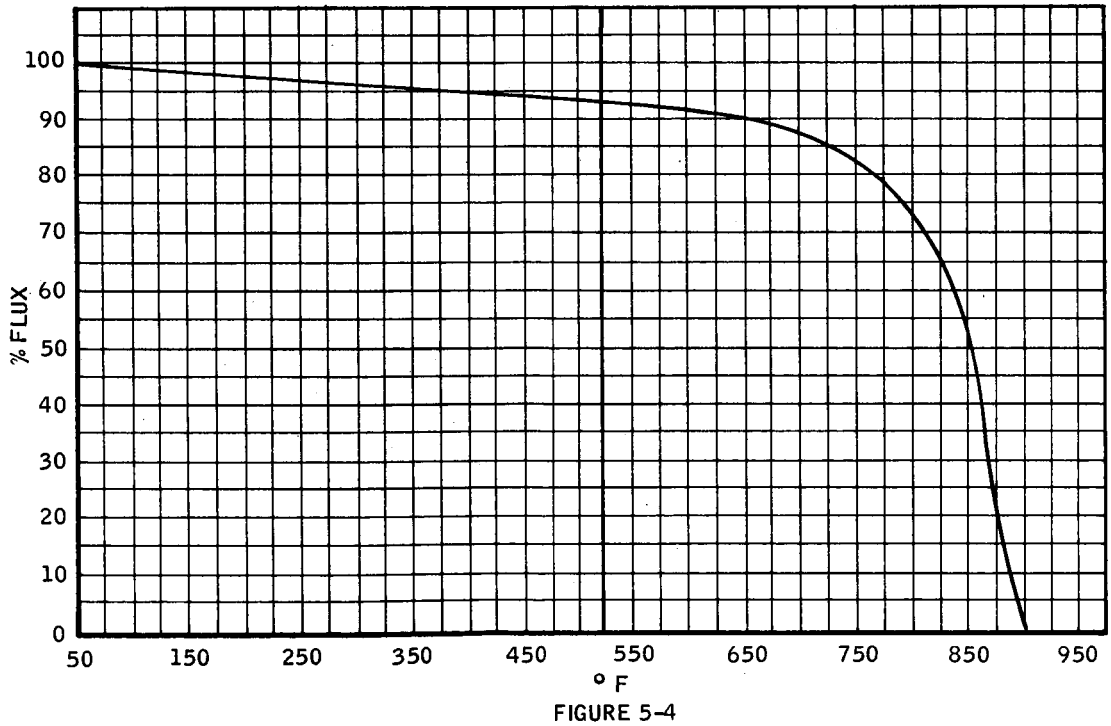

FIGURE 5-4

PERCENT FLUX RETAINED AFTER EXPOSING MAGNET TO TEMPERATURE SHOWN

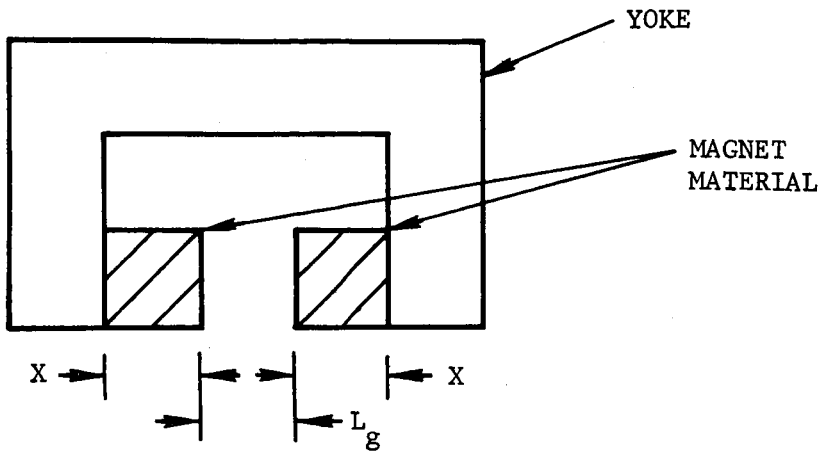

FIGURE 5-5

In the configuration of Figure 5-5, the area of the magnet is equal to the area of the gap, or

$$A_m = A_g \quad . \tag{5-1}$$

Using the equations presented by Thomas and Skinner,[7] the magnet relationships can be expressed by

$$L_m = \frac{f H_g L_g}{H_d} \tag{5-2}$$

and,

$$A_m = \frac{F B_g A_g}{B_d} \tag{5-3}$$

where

L_m = Total magnet length (cm)

A_m = Magnet cross sectional area (cm^2)

L_g = Length of gap (cm)

A_g = Area of gap (cm)

f = Reluctance factor

F = Leakage factor

B_g = Required gap flux density (gauss)

H_g = Gap Demagnitizing Force (oersteds)

B_d = Flux density in the magnet (gauss)

H_d = Corresponding Demagnitizing Force in the magnet for B_d (oersteds)

But since

$$\mu = \frac{B_g}{H_g} \quad , \tag{5-4}$$

where μ is the permeability of the gap medium, and for the non-magnetic material in the gap, $\mu = 1$ then

$$B_g = H_g \quad . \tag{5-5}$$

Using the dimensions which fit both the ion source and analyzer housing interfaces,

$L_m = 1.523$ cm .

From Equation (5-2)

$H_d = 100\ f$ (oe)

Assuming a reluctance factor (ratio of MMF of circuit to MMF of gap) of 1.5, then

$$H_d = 1500 \text{ oe} \tag{5-6}$$

From the demagnitization curve in Figure 5-3, the magnet flux density is thus seen to be

$$B_d = 4800 \text{ gauss} \tag{5-7}$$

For the particular arrangement of magnet and yoke being used, the leakage factor can be computed using the formula

$$F = 1 + \frac{L_g C_x}{A_g}\left[\frac{x}{0.875x + 1.3\ L_g} + \frac{0.34\ L_g}{x}\right] \tag{5-8}$$

where

x = length of one of the magnet pieces (cm)

C_x = perimeter of a cross-section of part x (cm)

However, combining Equations (5-1) and (5-3), it is seen that the leakage factor should be no greater than

$$F = 4.8 \tag{5-9}$$

Therefore, substitution into Equation (5-8) gives the result that

$$\frac{C_x}{A_g} = 2.58 \tag{5-10}$$

Using a circular magnet as a pole piece, the circumference to area ratio is thus

$$\frac{C_x}{A_g} = \frac{2}{R_m}$$

where R_m = magnet radius (cm)

and thus

$$R_m = 0.775 \text{ cm}$$

The diameter of the magnet required is thus 0.61 inch. Further consideration indicated that the magnet gap could be reduced to 0.540 inch. The following dimensions were then used for obtaining the Placovar magnets:

$$L_m = 0.600 \text{ inch}$$

or

$$x = 0.300 \text{ inch} \quad \text{and}$$

$$R_m = 0.300 \text{ inch} \quad .$$

To gain simplicity in the design, the magnet yoke was combined with the ion source mounting ring, as seen in Figure 5-1. This ring was made of Armco iron in order to obtain high permeability and low leakage. Further calculations showed that by using 0.150 inch thick material for the yoke in this configuration, then the field strength in the gap would suffer only a negligible loss.

5.2 TIME RESPONSE

The time response of the ion source and analyzer was computed using the program described in Section 3.4 and shown in Appendix A. For the system using a one liter per second pump, and having an effectively open ionizing region to the external atmosphere, the ion source reaches 95 percent of its final value (3 time constants) in 0.0025 seconds. The source time constant is thus

$$\tau_s = 833 \ \mu\text{-seconds}$$

for a step change in the external environmental pressure.

The program was then used to analyze the ion source and analyzer pressures as a function of time for step changes in the external pressure, from 1×10^{-8} to 1×10^{-2} torr and back to 1×10^{-8} torr, in half second intervals over a five second time period. Figure 5-6 shows the ion source pressure response as a function of these changes in the external pressure. Figure 5-7 similarly shows the analyzer pressure response.

For use of the system without a pump, the program given in Appendix B was utilized. Figure 5-8 shows the ion source response to the changes in the external pressure, and Figure 5-9 shows the analyzer pressure response.

These data were taken in order to analyze the effects present in the ion source as the spacecraft tumbled through the outside atmosphere. It clearly shows that the use of a pump benefits the system in the pressure build-up of both the ion source and the analyzer. Thus, more accurate atmospheric analysis over a wider dynamic external pressure range would result.

5.3 MECHANICAL CONSIDERATIONS

The mechanical design of the high pressure ion source was accomplished with two goals:

a. To achieve the dimensional requirements as derived in the theoretical analysis.

b. To simplify the mechanical arrangement of the electrodes for reproducibility, ease of assembly, and reducing the occurrance of shorted electrodes.

To meet the goals, the final design as shown in Figure 5-1 evolved. The mechanical assembly of the source involves two alignments, and ten screws holding the various electrodes to the mounting block. This mounting block contains the electron entrance and ion exit aperture, and serves as both the electron and ion accelerators. It mounts by a dowel-pin-type arrangement to the ion source mounting ring by two screws. The mounting ring is the yoke for the magnets which press into it. Four holes, compatible with the previously built quadrupole analyzers are provided for mounting the ring to the mass spectrometer. The feature of this arrangement is that the completed ion source can be aligned to the analyzer and removed many times without disturbing this alignment. The only part of the source remaining within the housing is the mounting ring containing the two permanent magnets. Four sub-assemblies are then mounted to the block; the filament assembly, the ion focusing system, the anode, and the repeller.

The filament assembly mounts the filament across two large metal blocks which are held with respect to each other by a suitable insulating media. In this application, each of these blocks is mounted to the filament shield with an insulating washer, such that the shield becomes the separation and locating media. A consequence of this mounting is that the filament heat is better utilized to heat and maintain the cleanliness of the source. In order to save critical spacing, this assembly is then mounted to the ion source block by the same two screws which hold the anode. The anode is electrically isolated from the screws however, which thread directly into the filament mounting blocks. Maintaining a gas seal in the mounting of the anode to the source block is also important. This is shown in the ionizing region cross-section illustrated in Figure 5-2.

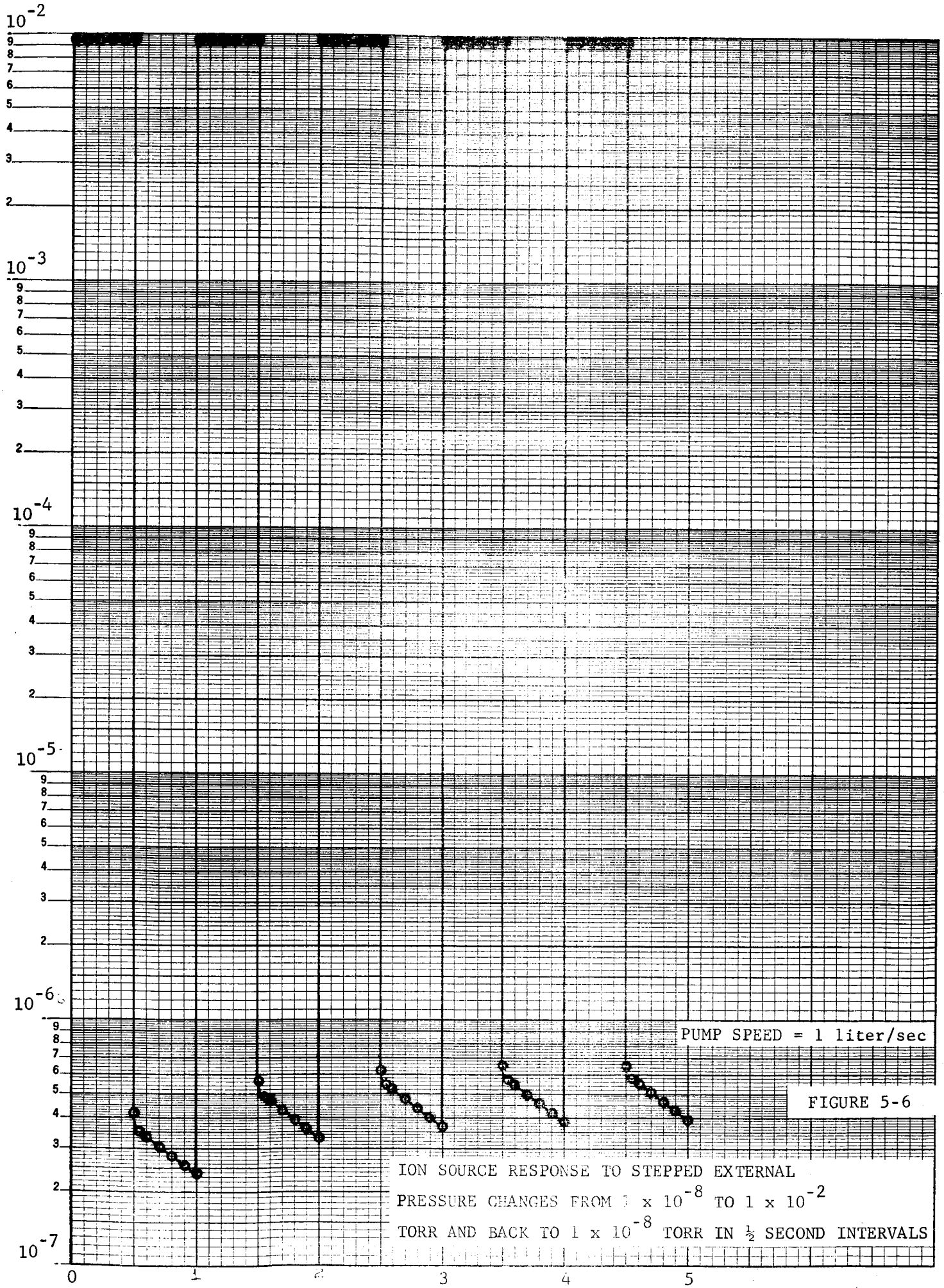

FIGURE 5-6

ION SOURCE RESPONSE TO STEPPED EXTERNAL PRESSURE CHANGES FROM 1 x 10^{-8} TO 1 x 10^{-2} TORR AND BACK TO 1 x 10^{-8} TORR IN ½ SECOND INTERVALS

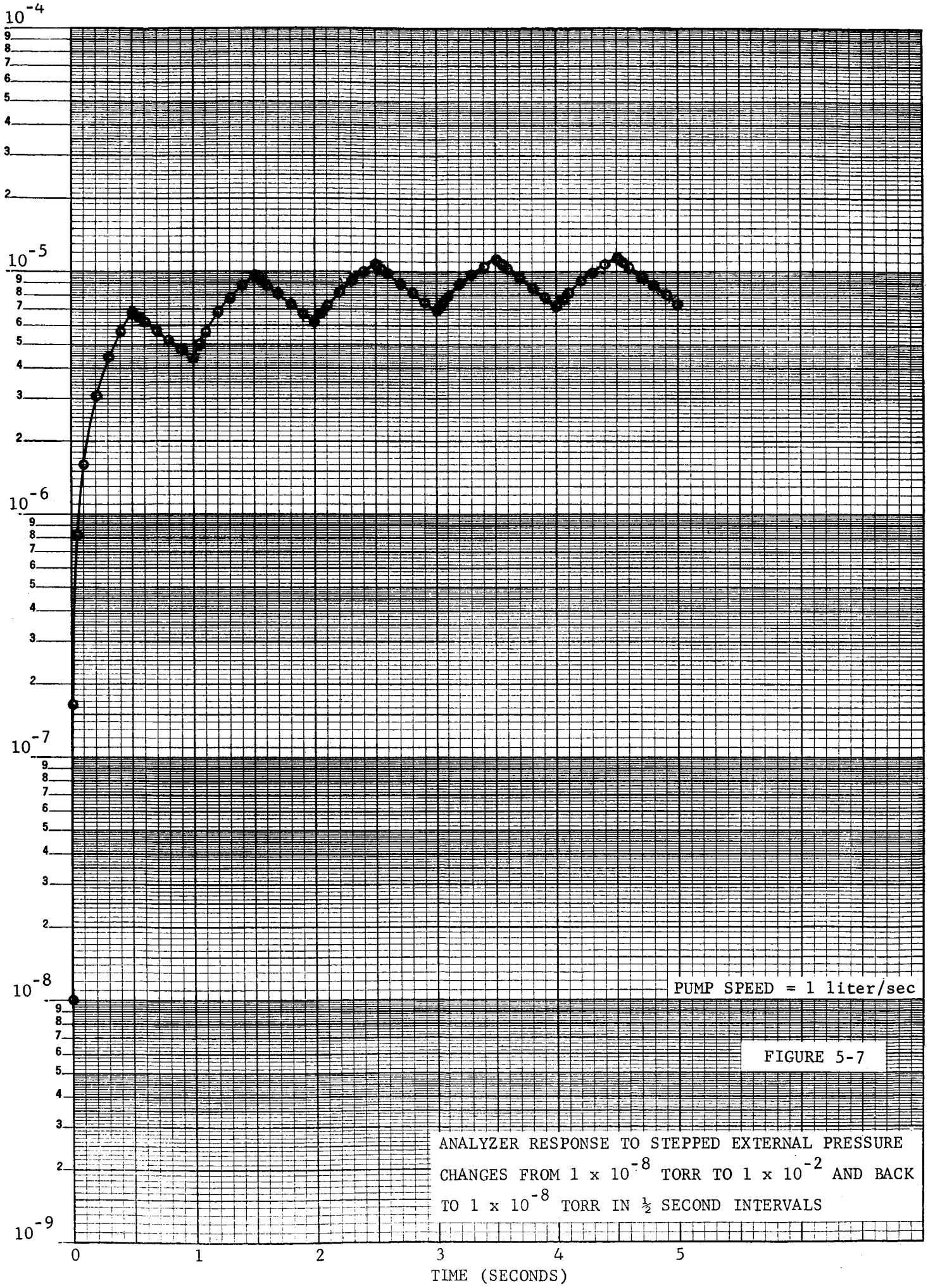

FIGURE 5-7

ANALYZER RESPONSE TO STEPPED EXTERNAL PRESSURE CHANGES FROM 1×10^{-8} TORR TO 1×10^{-2} AND BACK TO 1×10^{-8} TORR IN $\frac{1}{2}$ SECOND INTERVALS

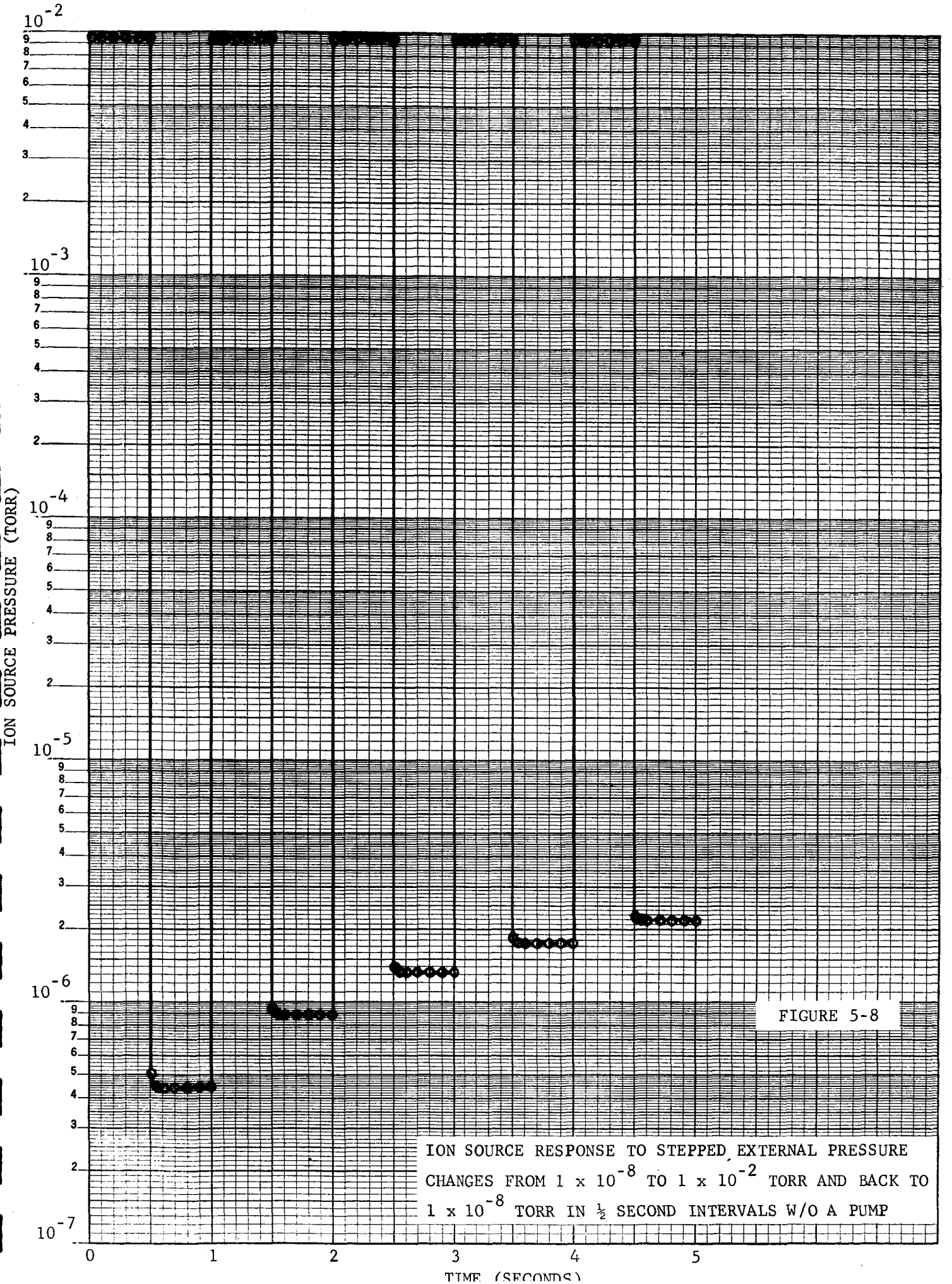

FIGURE 5-8

ION SOURCE RESPONSE TO STEPPED EXTERNAL PRESSURE CHANGES FROM 1×10^{-8} TO 1×10^{-2} TORR AND BACK TO 1×10^{-8} TORR IN ½ SECOND INTERVALS W/O A PUMP

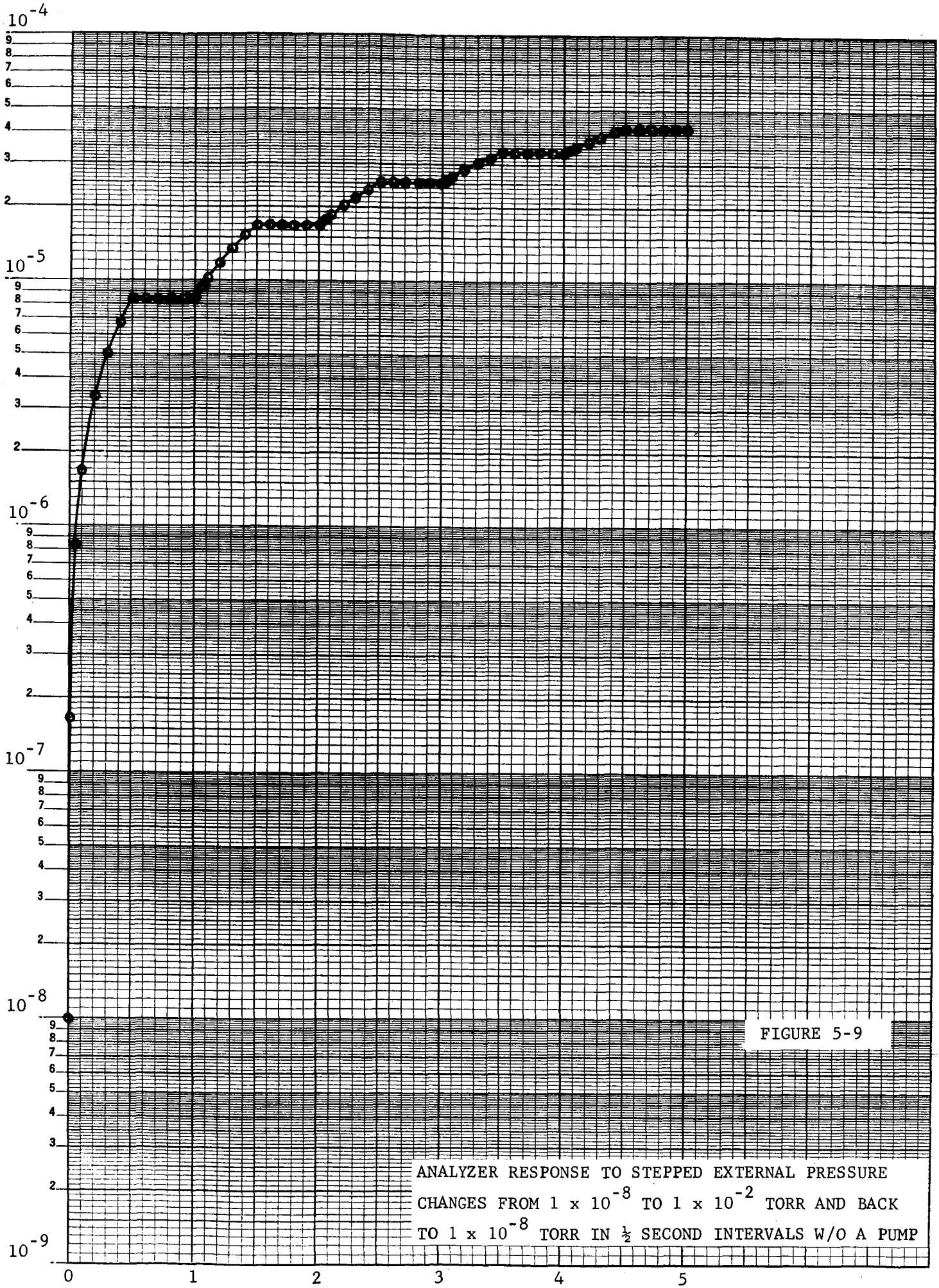

FIGURE 5-9

ANALYZER RESPONSE TO STEPPED EXTERNAL PRESSURE CHANGES FROM 1 x 10^{-8} TO 1 x 10^{-2} TORR AND BACK TO 1 x 10^{-8} TORR IN ½ SECOND INTERVALS W/O A PUMP

The ion focusing system consists of stacked electrodes insulated by ceramic washers. These are compressed against the mounting block by the mounting of the ion exit nozzle to the block. The nozzle is a defined interface into the quadrupole analyzer, but in this case, additional holes are provided through the sides of the nozzle to keep the ion focusing area in the low pressure area of the instrument. The ion focus system utilizes a single lens between the accelerator and nozzle to form a three element focal system. This lens is then split in the preferred orientation to compensate for ion source mass discrimination as described in Section 3.3.

The repeller in this design serves two functions, (1) an ion extraction electrode, and (2) the gas inlet system to the ionizing region. As seen in Figures 5-1 and 5-2, a blind hole is drilled down the repeller to a point at which two orthogonal holes meet it. The inlet gas flow enters the ionizing region through this system. The repeller is then isolated from the source block by a ceramic plate which provides both electrical insulation and gas sealing. Removal of the repeller only involves the unfastening of two screws. This enables inspection of the alignment of the apertures and lenses of the ion focusing system.

6. TEST RESULTS

The performance testing of high pressure ion source was divided into the three areas listed below:

a. Electron current tune-up

b. Ion current tune-up

c. Output current linearity with respect to ion source pressure.

To accomplish this task, the ion source was mounted in the prototype Specialized Mass Spectrometer. This tube was fabricated for Goddard Space Flight Center on the NASA Contract NAS5-3453, Item A. The use of this instrument properly simulated the actual use of the source.

The initial measurements on the ion source consisted of two axial field plots of the magnetic field. The flux density of the field was plotted down the ion source and quadrupole axis, and also down the axis of the magnets, with data recorded one inch away from the magnet center. Both axes are not the same since it was necessary to offset the magnets to accomodate the filament assembly. These two field plots are illustrated in Figures 6-1 and 6-2. While the field flux density of 1550 gauss was greater than anticipated, only the electron beam height, t', and the walking angle of the beam, θ, were effected. Adequate margin in the beam width relative to the ion exit aperture diameter allowed using the magnet as charged.

The quadrupole analyzer was then assembled with the high pressure ion source and mounted on a vacuum system for testing of the electron current transmission parameters. The test electronics were then set up in the configuration illustrated in Figure 6-3.

The originally installed filament was a 0.005 inch diameter wire of 75 percent Tungsten - 25 percent Rhenium alloy, and was aligned directly with the center line of the electron entrance aperture. At an analyzer pressure of 2×10^{-7} torr, the filament was turned on and a standard filament burn-in procedure employed. The results at this point appeared to be quite normal, so the source was then reconnected to obtain anode current. None was obtained regardless of voltage variations, so the source was then removed and disassembled for inspection. It was observed that the filament had bowed approximately 0.010 inch from the center line of the accelerator slit. A new filament of the same material was then installed and aligned, and the source was pumped down.

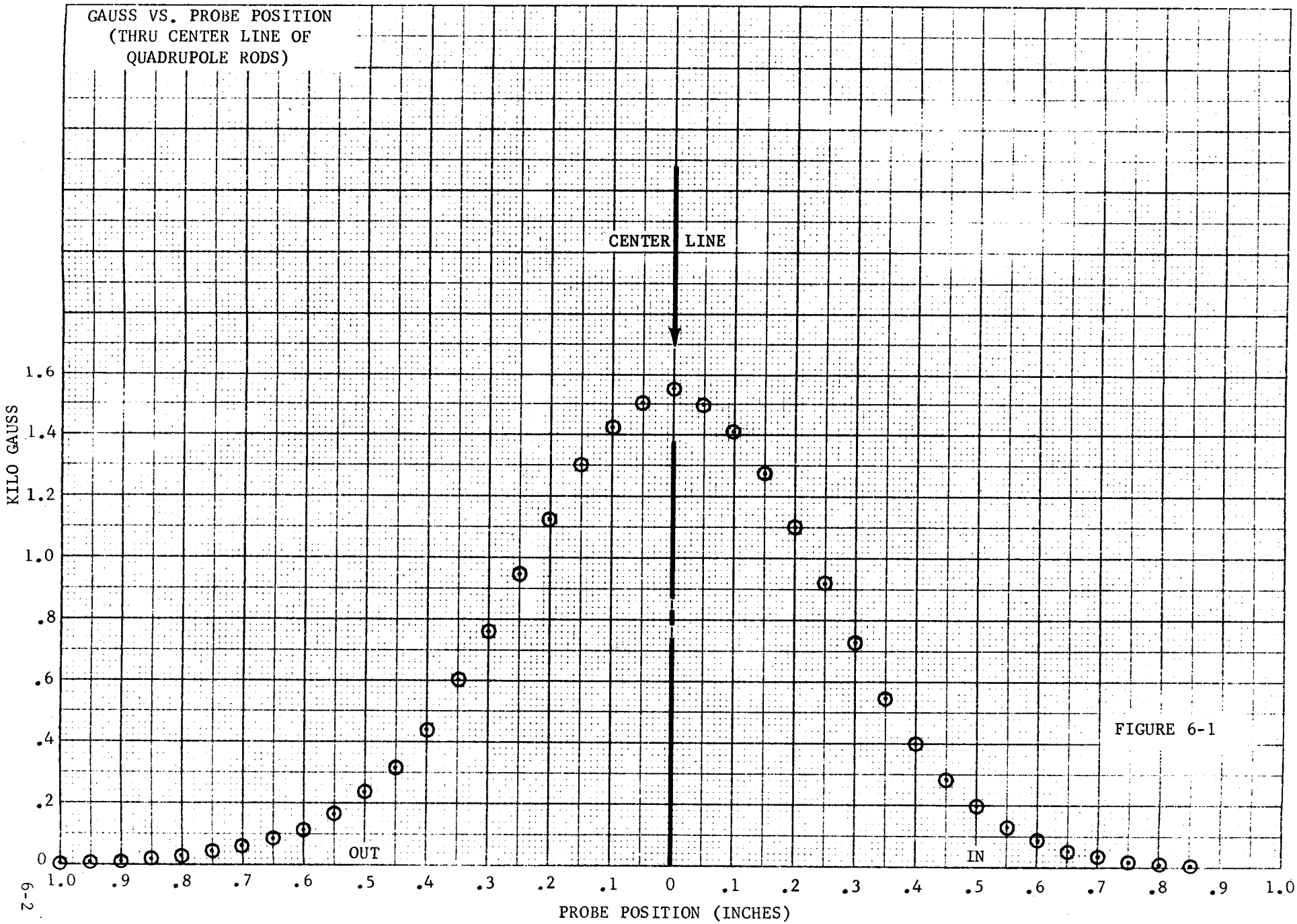
GAUSS VS. PROBE POSITION
(THRU CENTER LINE OF
QUADRUPOLE RODS)
CENTER LINE
KILO GAUSS
1.6
1.4
1.2
1.0
.8
.6
.4
.2
0
OUT
IN
1.0 .9 .8 .7 .6 .5 .4 .3 .2 .1 0 .1 .2 .3 .4 .5 .6 .7 .8 .9 1.0
PROBE POSITION (INCHES)

FIGURE 6-1

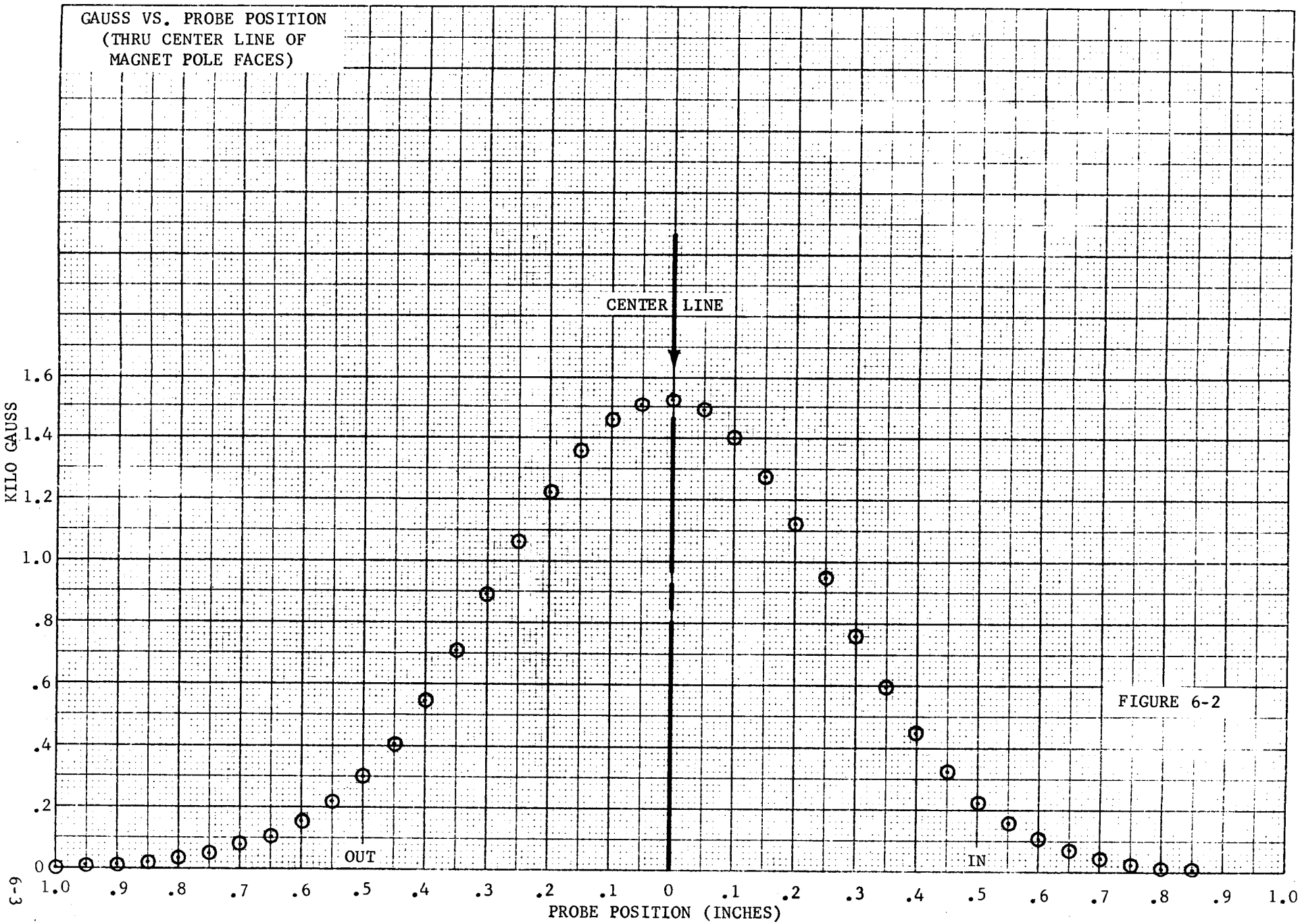

FIGURE 6-2

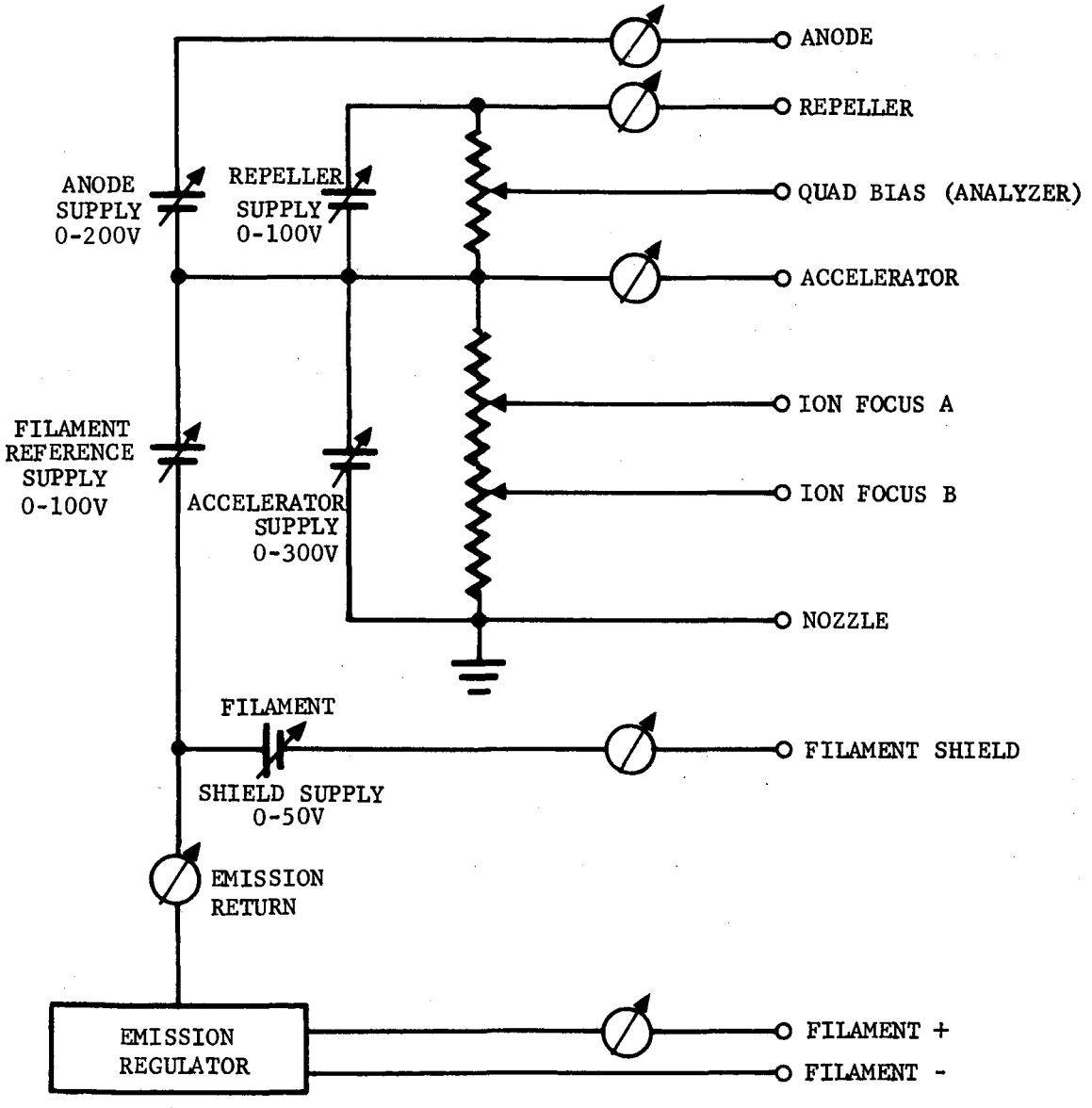

FIGURE 6-3

Electronics Test Set Up

When this filament was turned on the results were identical. The filament had, again, moved away from the acelerator slit and no anode current could be obtained.

A coiled filament was then constructed using 0.005 inch diameter wire (25 percent Tungsten and 75 percent Rhenium) wound on a 0.007 inch diameter form. This filament was installed and aligned so three coils were distributed over the length of the entrance aperture. With this arrangement, 4 microamperes of anode current was achieved while obtaining a total emission current of 200 microamperes. After a short time, this decayed to 2×10^{-8} amperes maximum regardless of the applied potentials.

The system was then analyzed to see if the changing filament position was a function of natural sag, or if the force applied by the filament current and the orthogonal magnetic field could be moving the filament from its aligned location. The filament polarity was thus reversed to determine if the magnetic field was applying enough force to tow the filament away from the accelerator slit. Again, the anode current was 4 microamperes as before, and this slowly decaded to an unacceptable value. The magnetic field was apparently causing the filament to move. To prove the above, a new filament (0.003 diameter coiled wire) was installed and turned on. No anode current was obtained as expected, and inspection revealed that the filament had moved 0.021 inch from the accelerator slit in the direction of the magnetic force. This force was then calculated using the values of 1500 gauss and 1.5 amperes of filament current, giving

$$F = 1.78 \times 10^{-2} \ \frac{\text{lb-ft}}{\text{sec}^2}$$

This force appeared comparable to the filament strength and was assumed to cause the movement of the filament.

In order to alleviate this problem, a ribbon filament was constructed of pure Rhenium, of dimensions 0.0015 x 0.010 inch, and was installed with the stiff direction parallel to the applied force. The anode current thus obtained was 1.5 microamperes out of a total current of 100 microamperes. The transmission efficiency in this case was lower, but it proved to be more reliable and more consistant. The filament current was held below 1.5 amperes.

From the results of an electrolytic tank investigation of the ion focusing system, it appeared that the tube lens effects created at the ion exit aperture would not seriously drop the sensitivity of the source by defocusing of the ion beam. Figure 6-4 illustrates a typical series of trajectories through the aperture. These indicate that while the ions entering near the edge of the aperture do undergo some defocusing, they refocus upon exiting the tube lens, thus keeping them within the boundary limits of the aperture walls. From these results, it appears reasonable that the 10 percent transmission efficiency of the ions assumed for Equation (4-18) is realizable.

The sensitivity tune-up of the ion source was accomplished by optimizing the ion output current over a range of repeller and filament reference supply potentials. The ion focus lenses were tuned to the maximum sensitivity in each case. This procedure developed the optimum ion source potential, V_r, of 46 volts and a filament reference supply potential of 30 volts. The anode current was 5 microamperes.

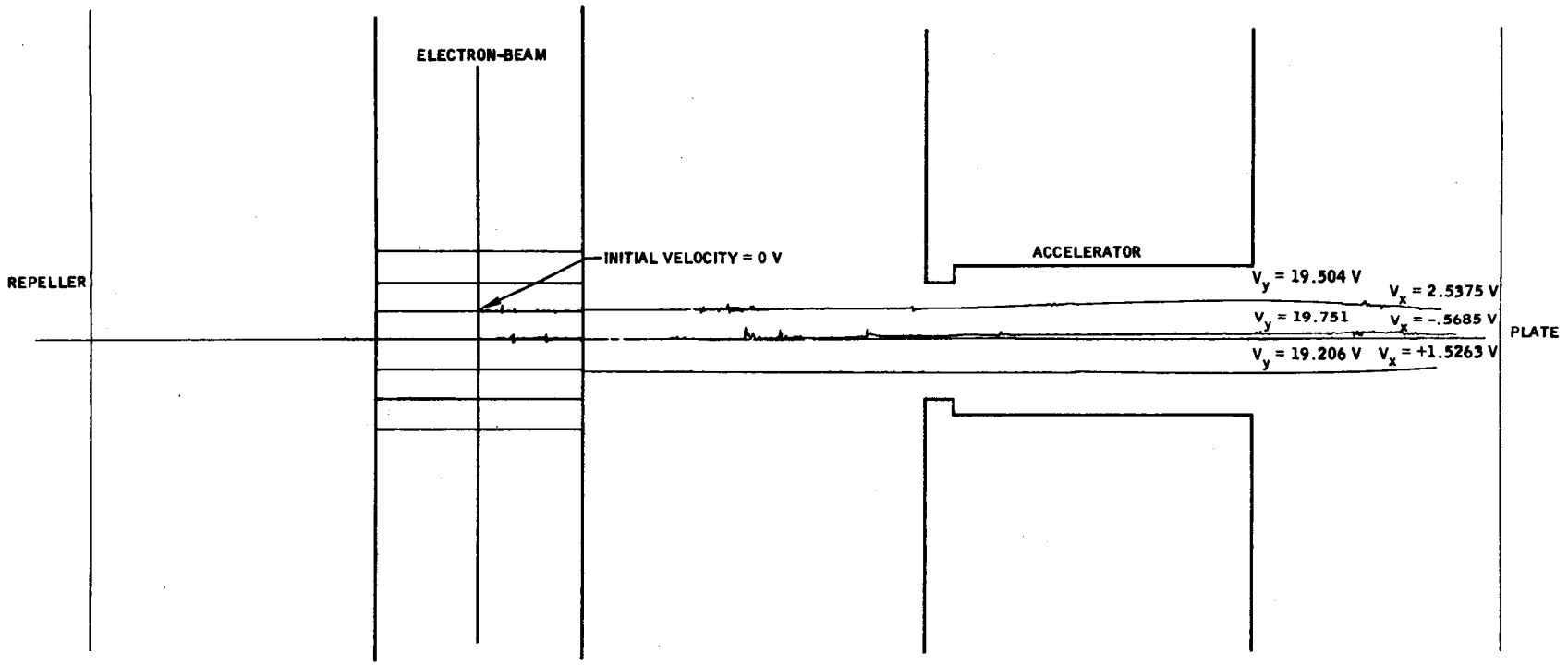
ELECTRON-BEAM
REPELLER
INITIAL VELOCITY = 0 V
ACCELERATOR
V_y = 19.504 V
V_x = 2.5375 V
V_y = 19.751
V_x = -.5685 V
V_y = 19.206 V
V_x = +1.5263 V
PLATE

FIGURE 6-4

The energy of the electrons upon ionization is described by Equation (4-24) which gives a value of V_{el} = 53 volts. These potentials give very close agreement with the theoretical calculations, and the sensitivity obtained was approximately 8×10^{-9} amps/torr for the m/e 28 peak of nitrogen. For the ion source testing, the analyzer was detuned to give a resolution of about $\Delta m/m = 1/10$ in order to avoid oscillator stability problems. A typical spectrum scan of the m/e 28-32 group at this resolution is shown in Figure 6-5.

The ion energy spread, ΔV_{ion}, was then measured by using an ion suppression technique by applying a bias to the quadrupole rods. This method was previously used in ion source tune-up during quadrupole analyzer testing. The initial results, as shown in Figures 6-6 and 6-7 show energy spreads of 25 volts for m/e 28, and 10 volts for m/e 4 (helium) respectively. These data appear to indicate that the energy spread is mass dependent, or that the quadrupole bias technique of measurement is voltage dependent since the two measurements were made at different V_{AC} potentials on the quadrupole. Figure 6-8 then illustrates the quad bias cutoffs for m/e 28 (N_2) and m/e 40 (Argon) at a V_{AC} = 255 volts (rms), and a repeat of the m/e 4 (helium) cutoff at a V_{AC} = 63 volts (rms). It appears that the observed energy spread is a function of the RF amplitude, since the two scans for m/e 28 and 40 are the same within experimental accuracy. Again, in Figure 6-9, the apparent energy spread for m/e 28 is shown for three different V_{AC} levels where they give different values. Thus, it appears that the quad bias cutoff technique is dependent upon the applied RF amplitude, and consequently is not an accurate method for determination of the ion source energy spread characteristic.

The ion source linearity versus pressure data was taken over the pressure range of 1×10^{-3} to 1×10^{-1} torr for three different sample gases; nitrogen, helium, and oxygen. The sample pressure was measured using a CEC Micromanometer which has an operating pressure range of 1 to 150 microns, and a reproducibility of 0.5 microns. Consequently, the accuracy of the pressure measurements at 1×10^{-3} torr was limited by the measuring equipment. Two linearity runs are presented for each of the samples. Figures 6-10 and 6-11 show the linearity results using a nitrogen sample with the quadrupole tuned to m/e 28. These curves show a non-linearity of less than 10 percent at 1×10^{-2} torr, the maximum designed pressure for the ion source. The data was taken, however, up to 1×10^{-1} torr in order to analyze the non-linearity at pressures higher than the design maximum. These data indicate that higher pressure levels can be tolerated by the ion source, and that calibration of the non-linearity will give sufficient accuracy of measurement. Figures 6-12 and 6-13 show the ion source m/e 4 output as a function of a helium sample pressure in the ionizing region, and Figures 6-14 and 6-15 illustrate the oxygen linearity. These curves, as expected, show a better linearity characteristic at the maximum designed pressure than for N_2. This improvement for He is due to the reduced ion space charge at the corresponding pressure of N_2. The ion source is thus capable of operating at higher pressure levels of He without experiencing large non-linearity.

The final operating conditions of the ion source pressure of N_2 are listed below for operation with a nitrogen or oxygen sample:

V (Accelerator) = 250.0 volts

V (Repeller) = 295.6 volts

V (Filament) = 220.1 volts

FIGURE 6-5
TYPICAL m/e 28-32 SPECTRUM SCAN

I_T = 90μa
I_i = 2μa
A_{CC} = 200 V
V_{AC} = 255 V
V_{DC} = 56 V (RP +)

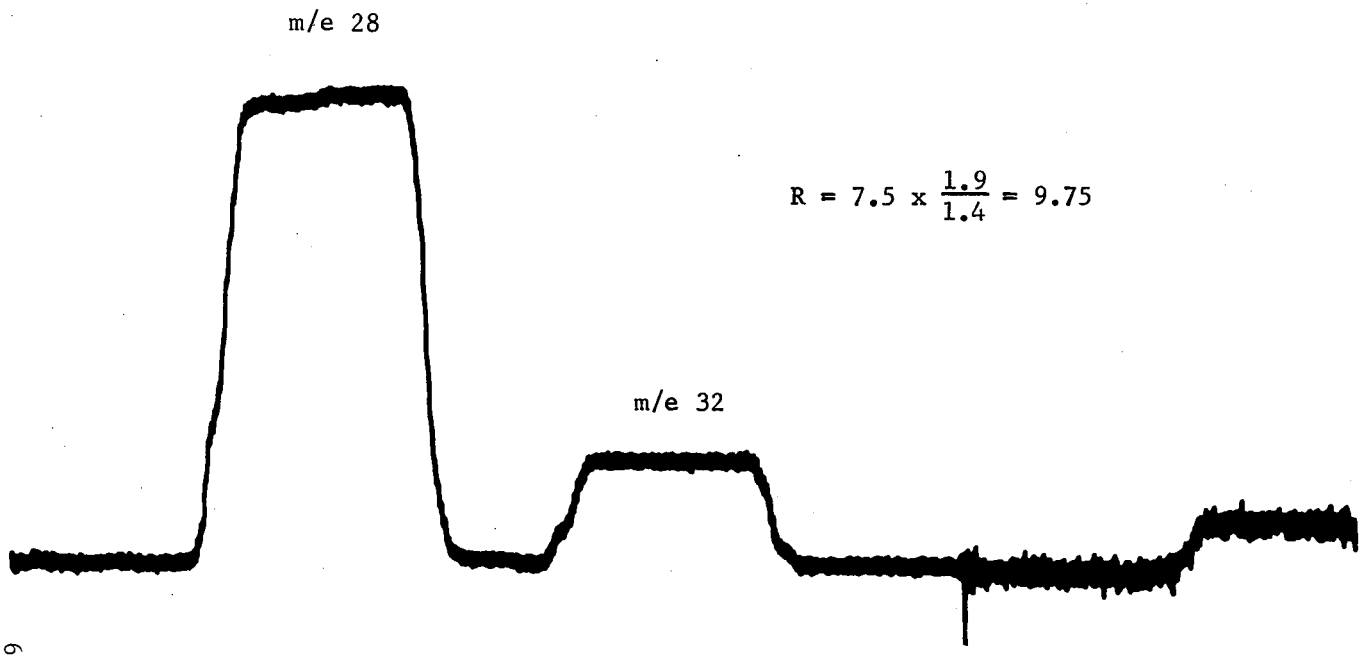

$$R = 7.5 \times \frac{1.9}{1.4} = 9.75$$

FIGURE 6-6

QUAD BIAS V_s I_{28}^+

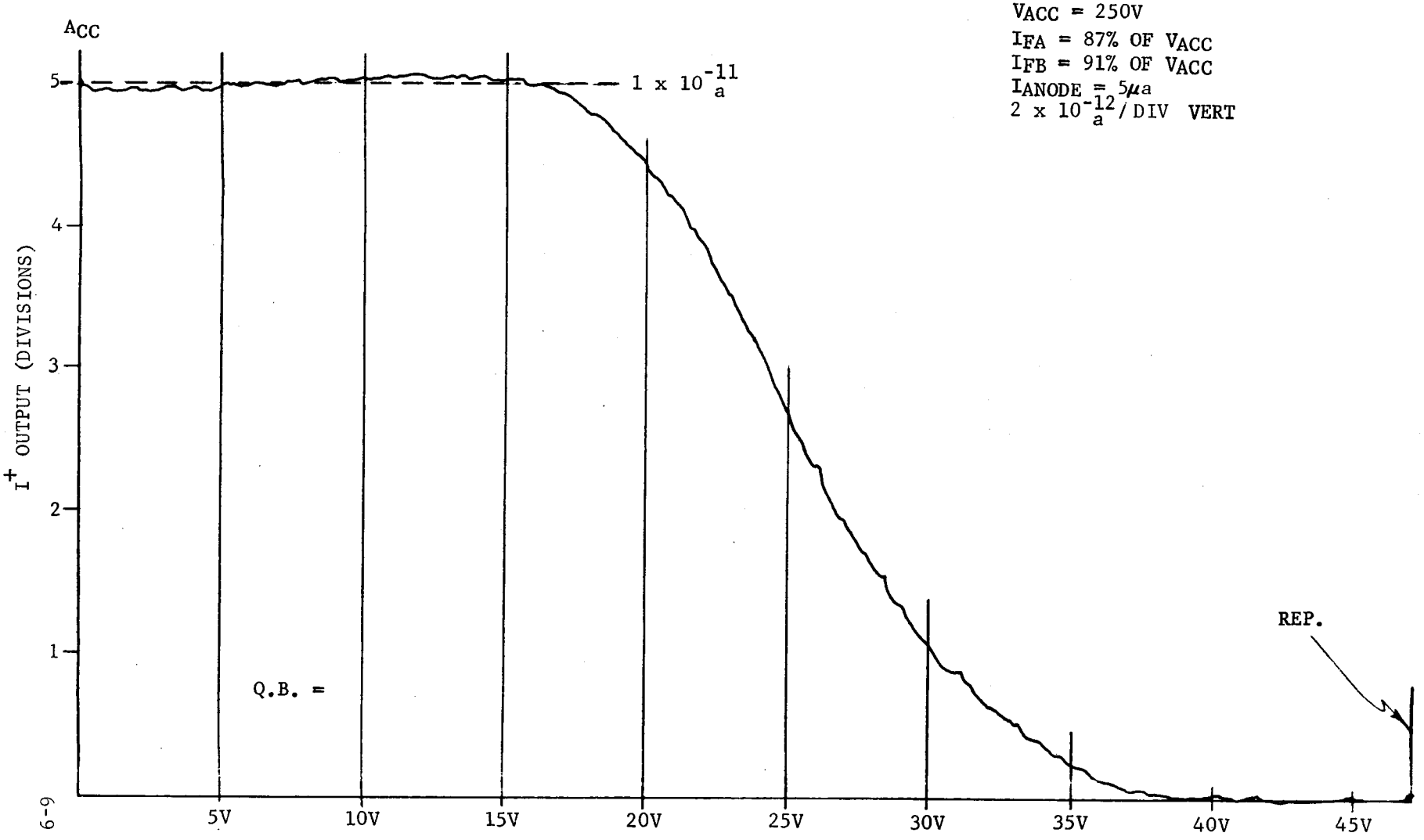

FIGURE 6-7
QUAD BIAS V_s I_4^+

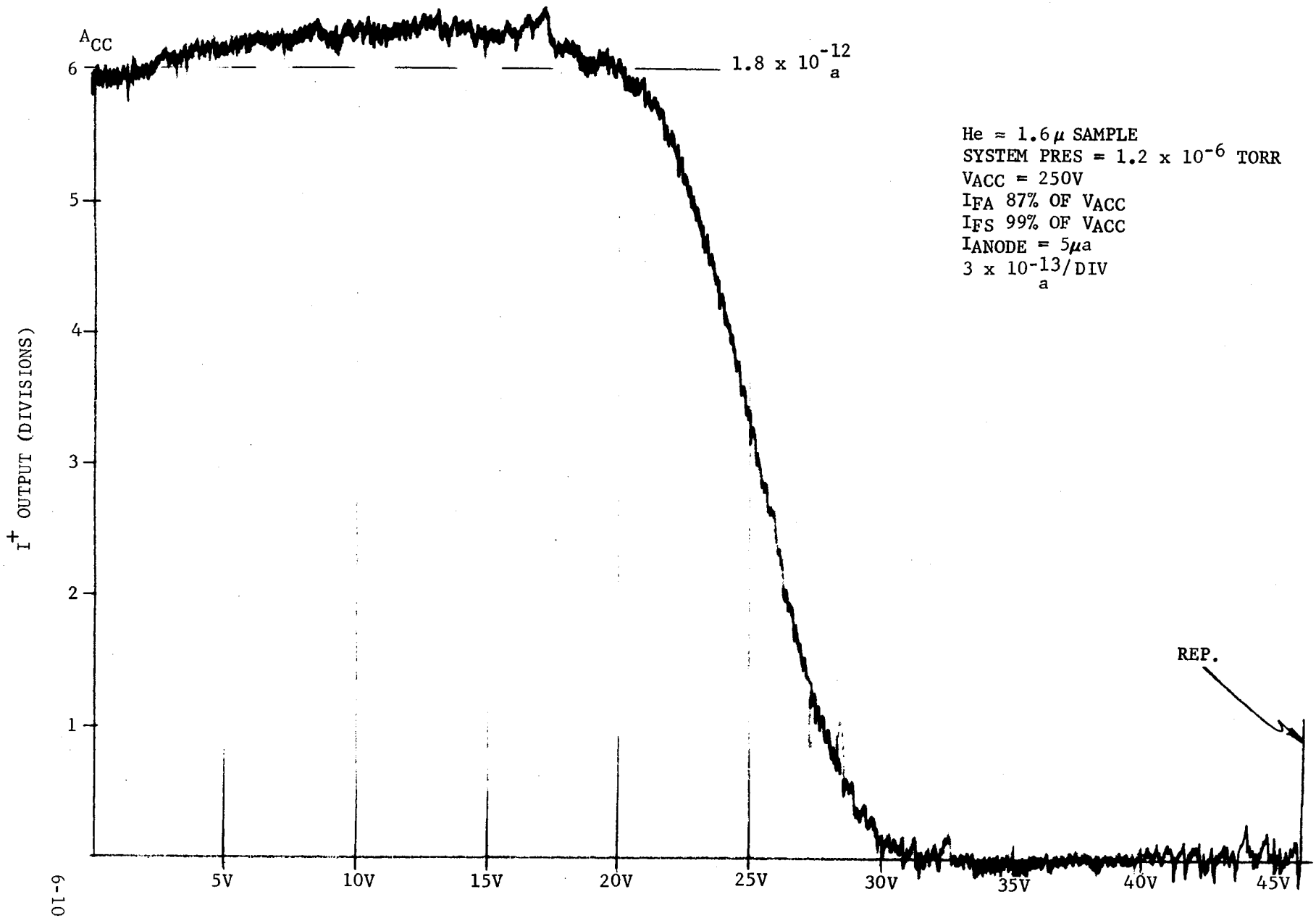

FIGURE 6-8
ION ENERGY SPREAD ANALYSIS

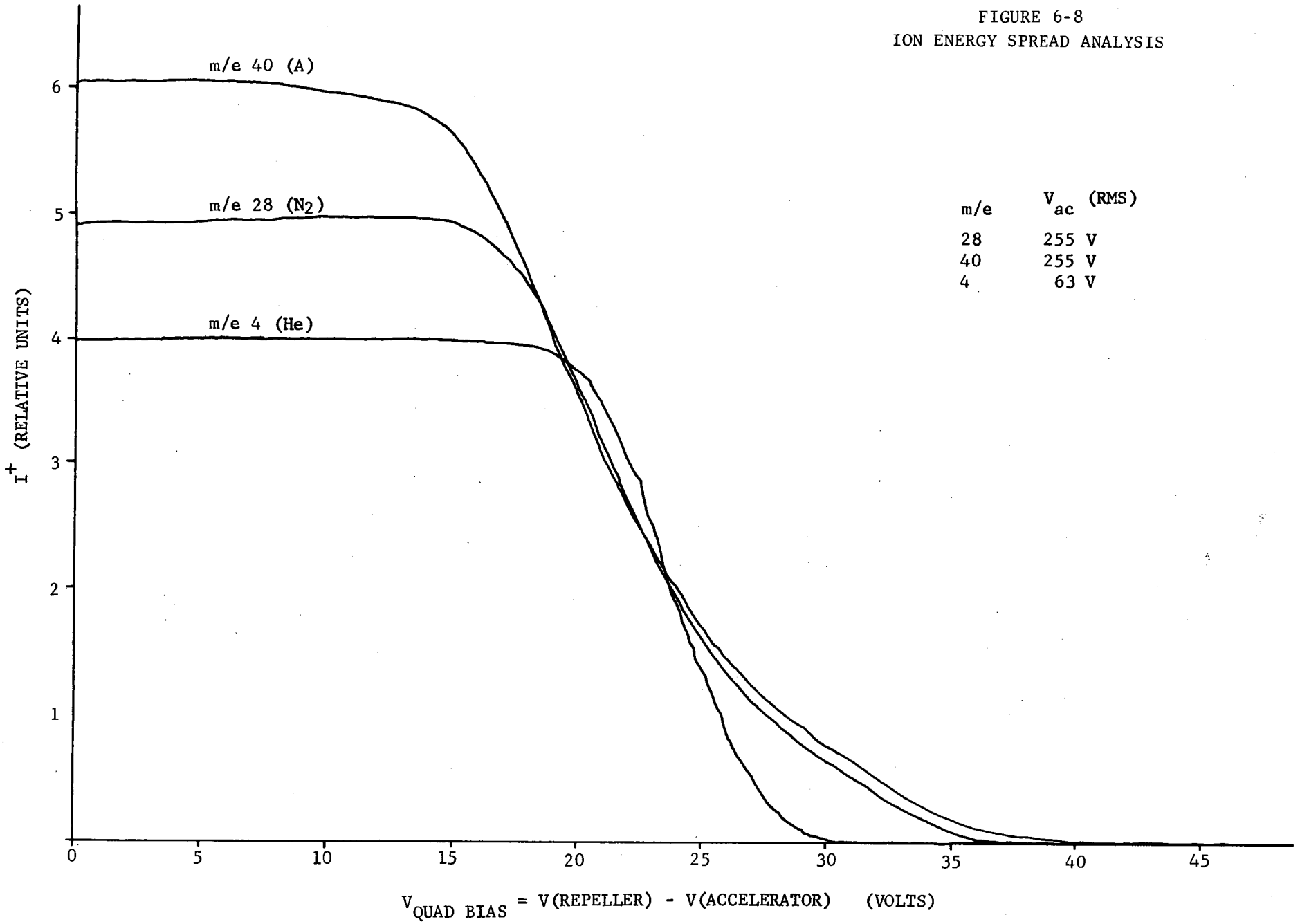

m/e	V_{ac} (RMS)
28	255 V
40	255 V
4	63 V

FIGURE 6-9
ION ENERGY SPREAD ANALYSIS

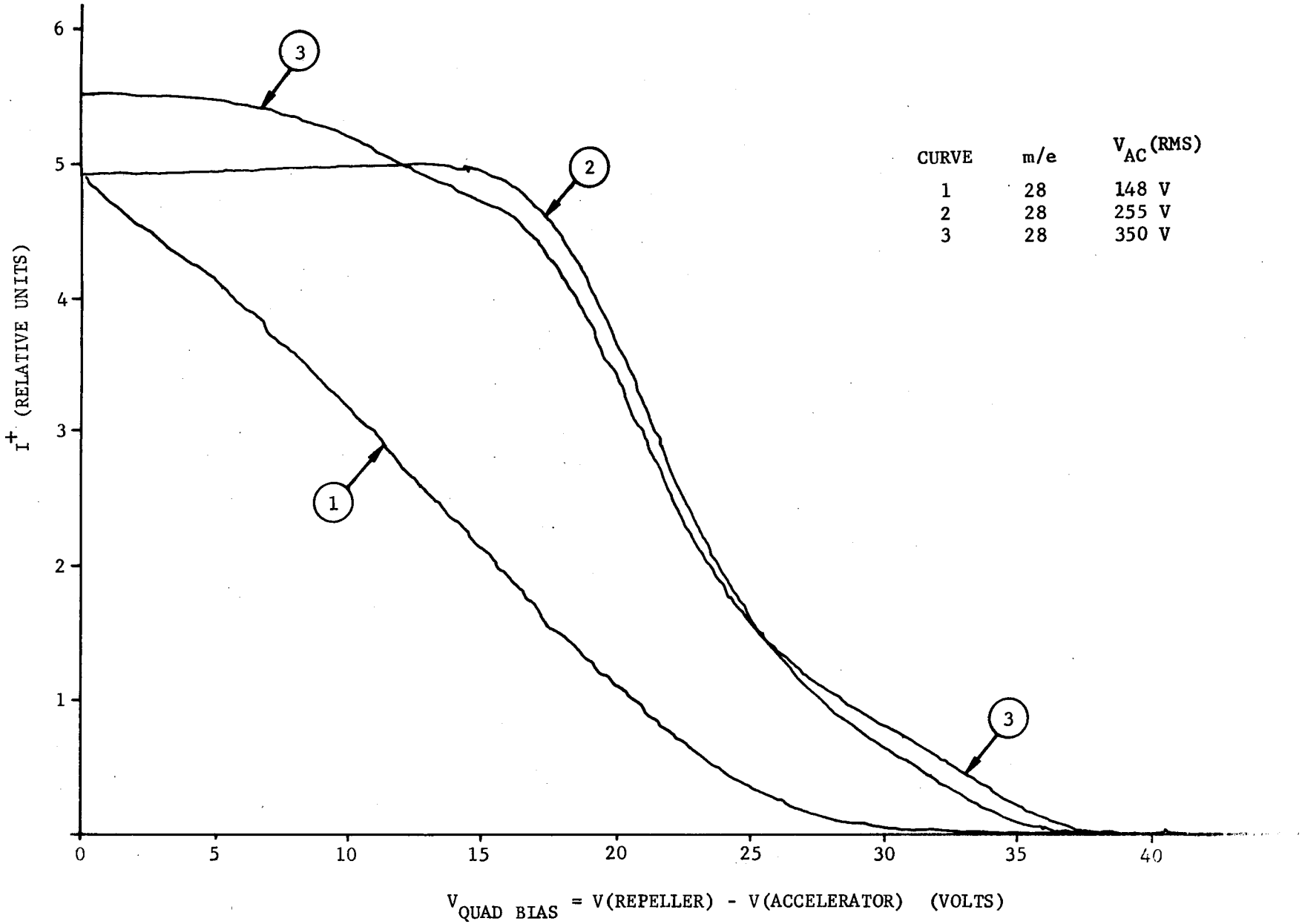

CURVE	m/e	V_{AC} (RMS)
1	28	148 V
2	28	255 V
3	28	350 V

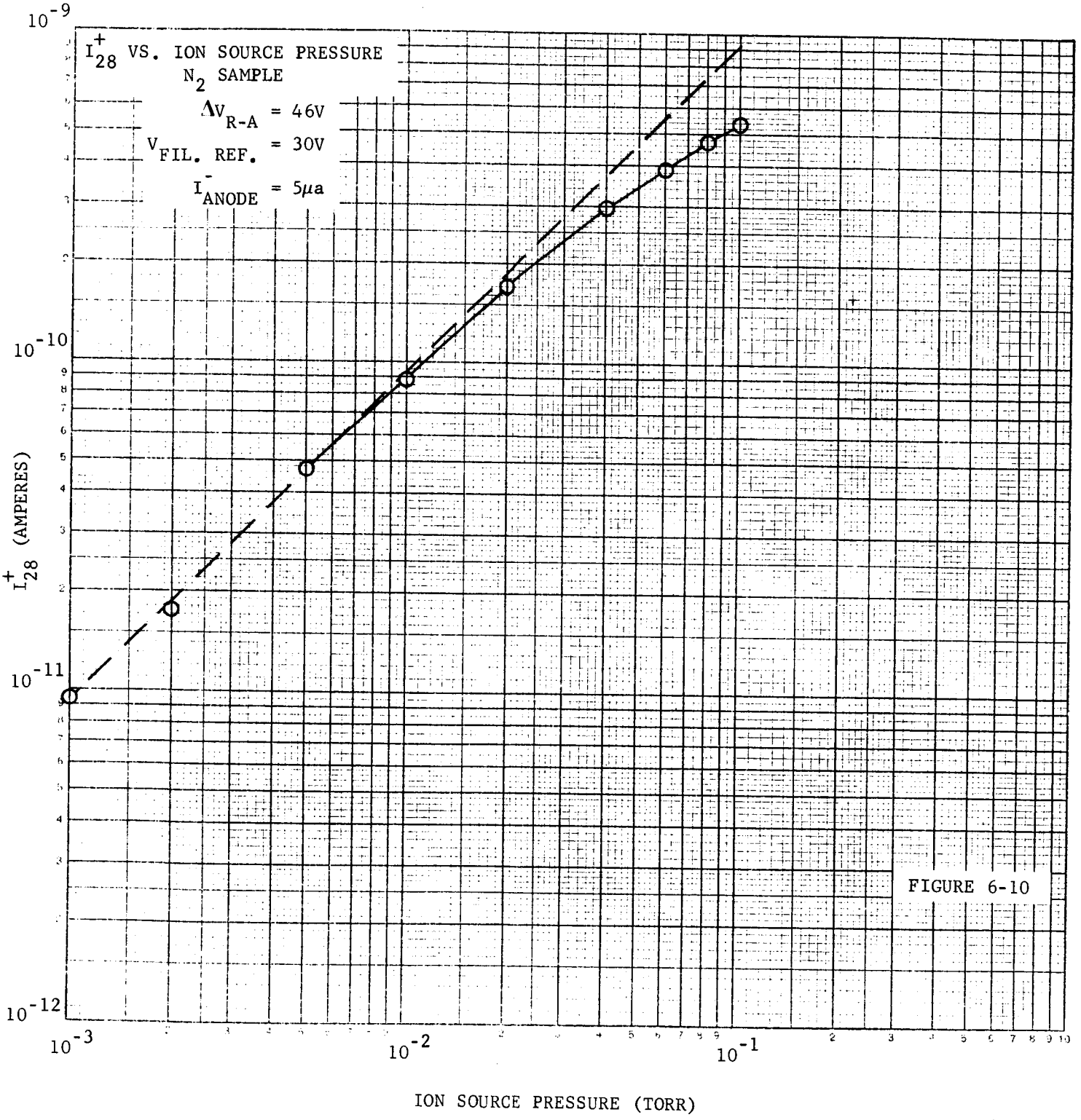
I^+_{28} VS. ION SOURCE PRESSURE
N_2 SAMPLE
ΔV_{R-A} = 46V
$V_{FIL.\ REF.}$ = 30V
I^-_{ANODE} = 5μa
10^{-9}
10^{-10}
10^{-11}
10^{-12}
I^+_{28} (AMPERES)
10^{-3}
10^{-2}
10^{-1}
ION SOURCE PRESSURE (TORR)

FIGURE 6-10

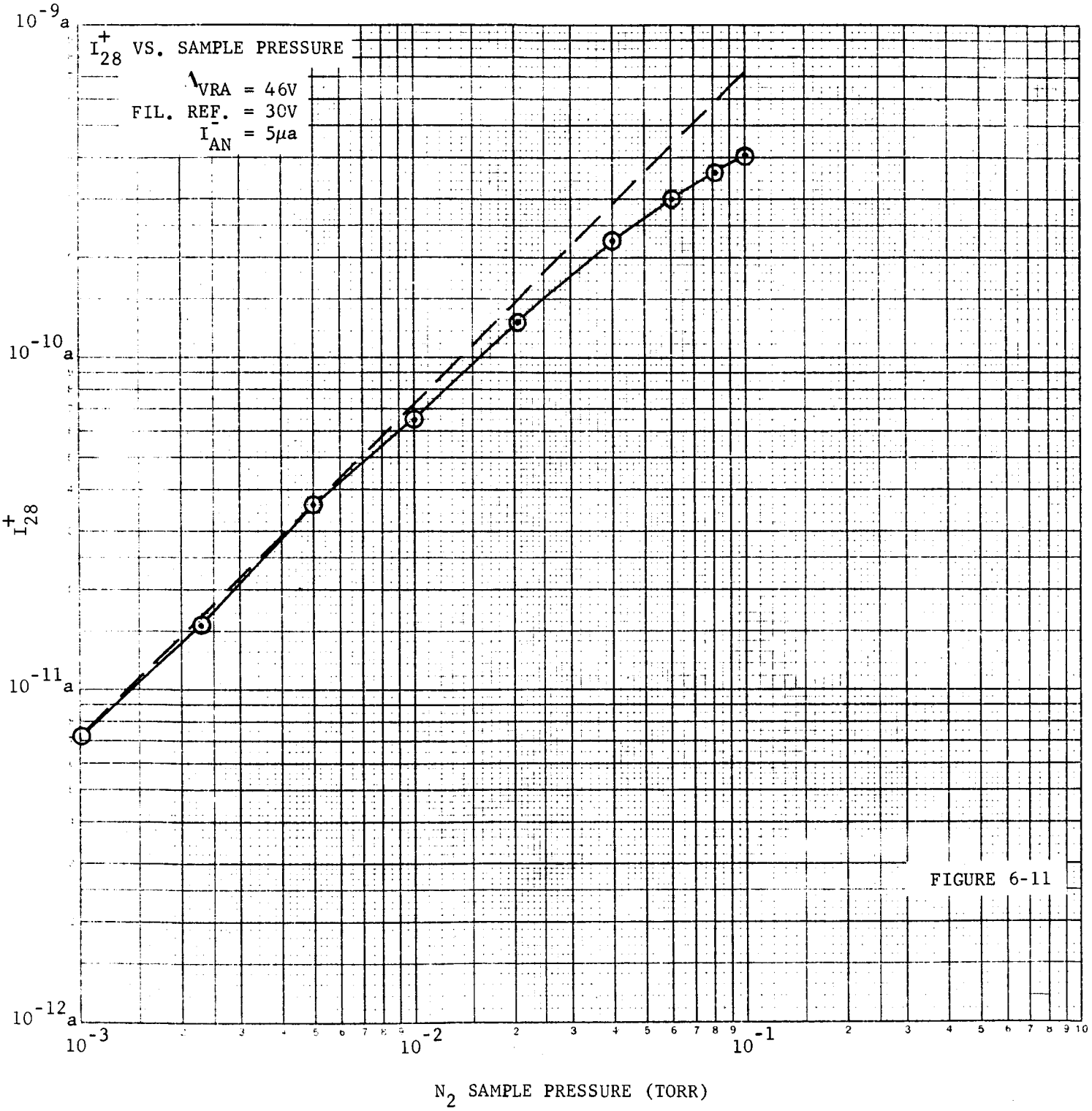
I_{28}^{+} VS. SAMPLE PRESSURE
V_{RA} = 46V
FIL. REF. = 30V
I_{AN} = 5μa
10^{-9}a
10^{-10}a
10^{-11}a
10^{-12}a
I_{28}^{+}
10^{-3}
10^{-2}
10^{-1}
N_2 SAMPLE PRESSURE (TORR)

FIGURE 6-11

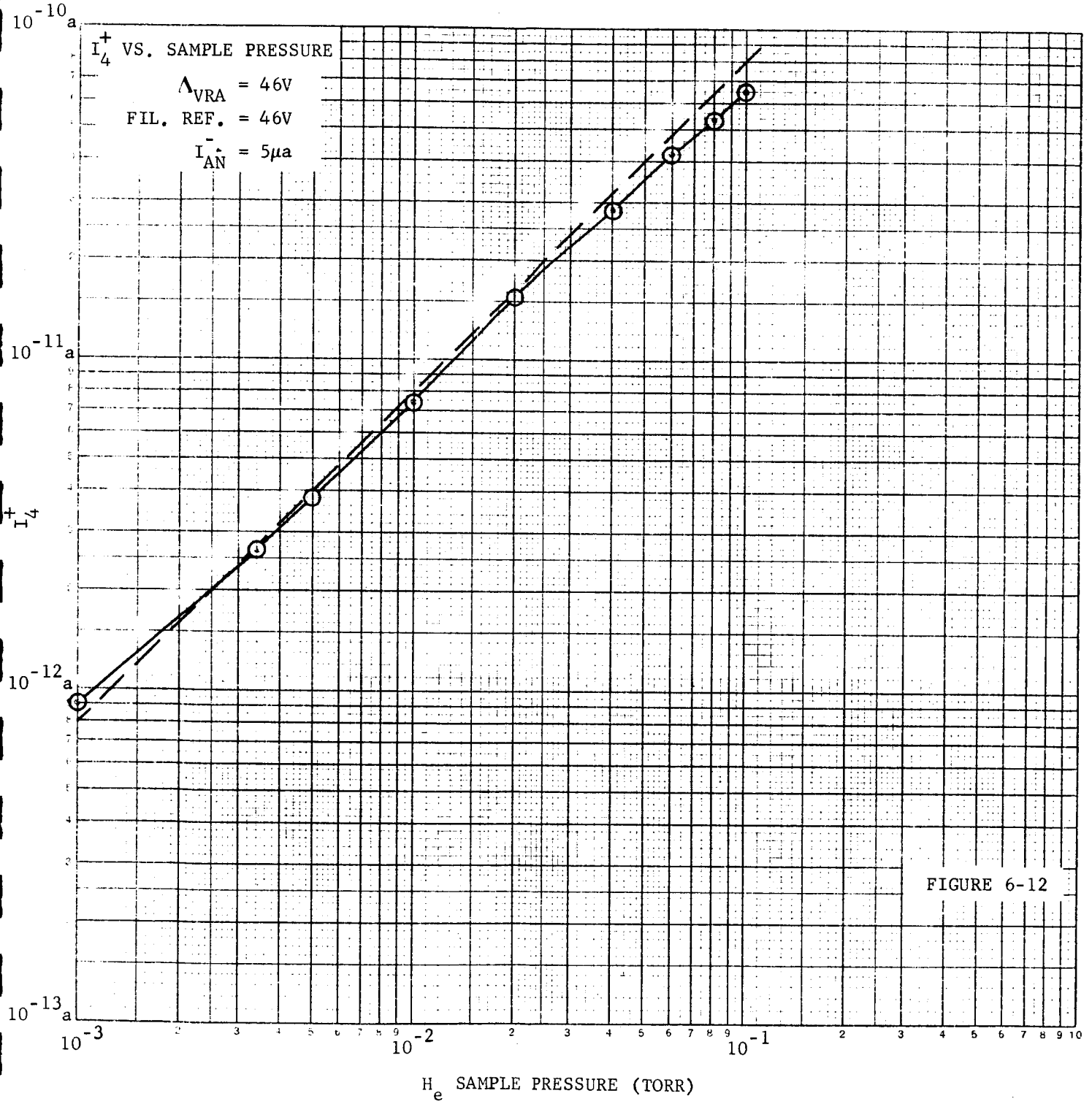
I_4^+ VS. SAMPLE PRESSURE
Λ_{VRA} = 46V
FIL. REF. = 46V
I_{AN}^- = 5μa
10^{-10}a
10^{-11}a
10^{-12}a
10^{-13}a
I_4^+
10^{-3}
10^{-2}
10^{-1}
H_e SAMPLE PRESSURE (TORR)

FIGURE 6-12

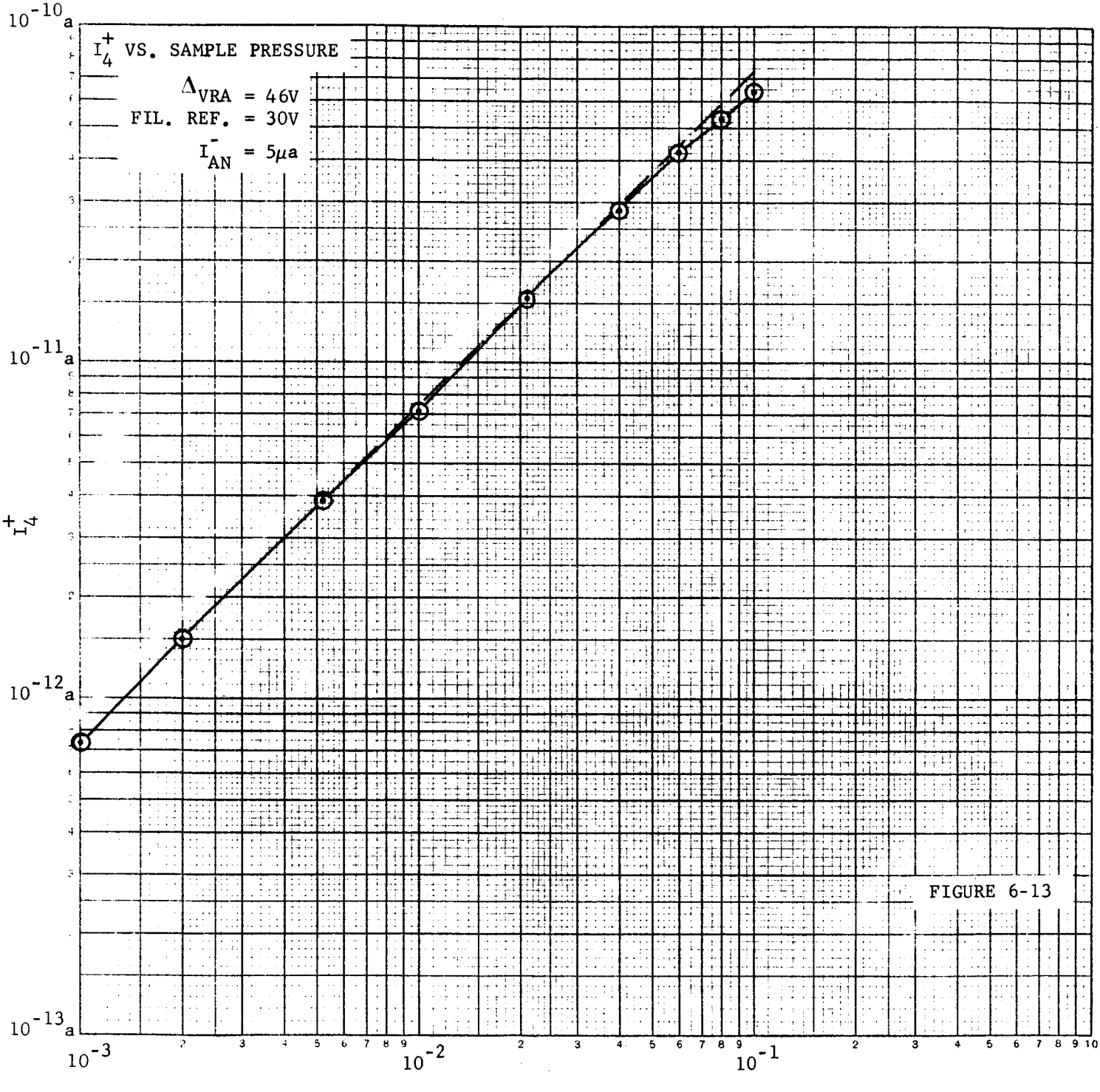
I_4^+ VS. SAMPLE PRESSURE
Δ_{VRA} = 46V
FIL. REF. = 30V
I_{AN}^- = 5μa
10^{-10}a
10^{-11}a
10^{-12}a
10^{-13}a
I_4^+
10^{-3}
10^{-2}
10^{-1}
H_e SAMPLE PRESSURE (TORR)

FIGURE 6-13

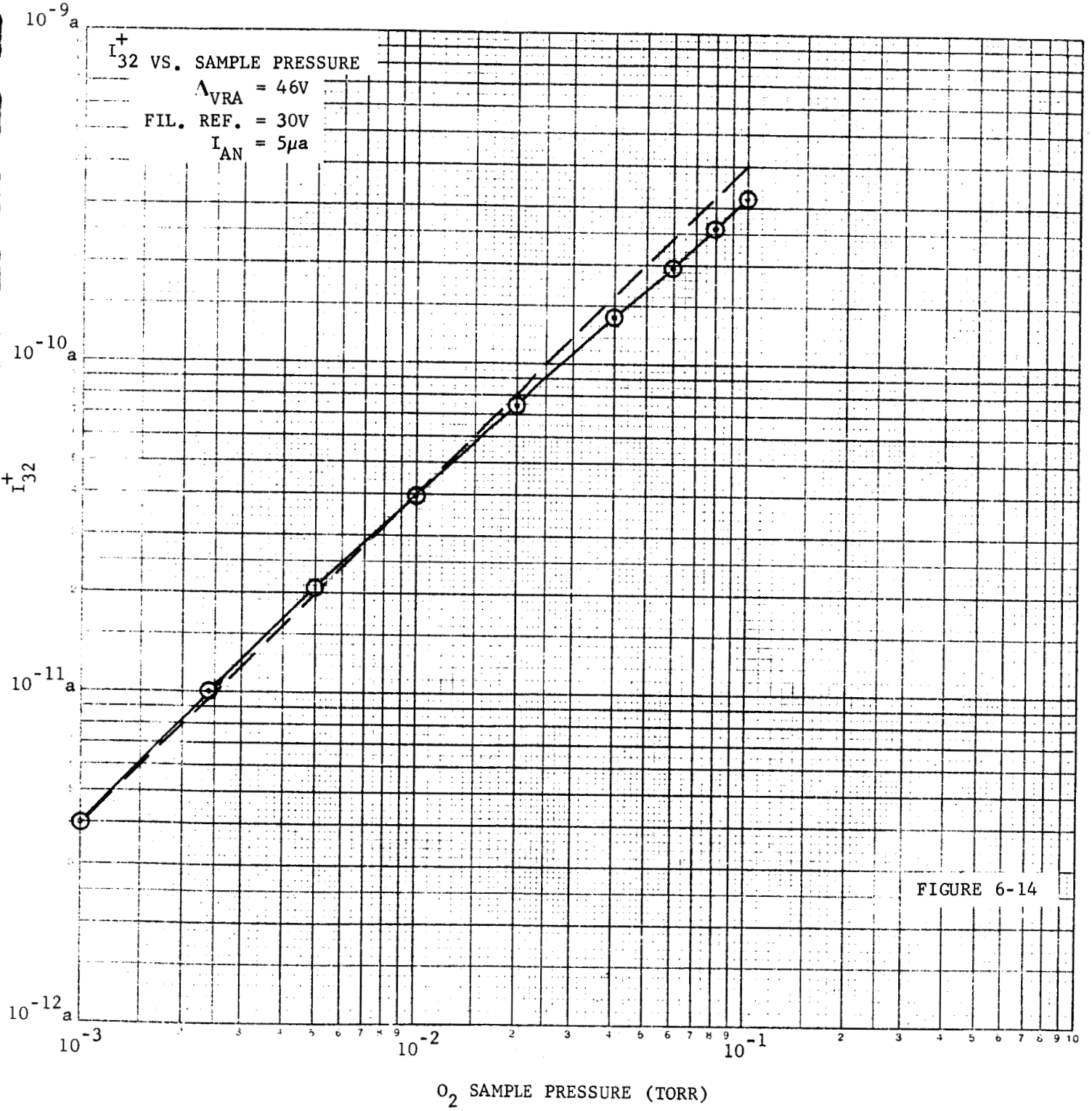
I^+_{32} VS. SAMPLE PRESSURE
Λ_{VRA} = 46V
FIL. REF. = 30V
I_{AN} = 5μa
10^{-9}a
10^{-10}a
10^{-11}a
10^{-12}a
I^+_{32}
10^{-3}
10^{-2}
10^{-1}
O_2 SAMPLE PRESSURE (TORR)

FIGURE 6-14

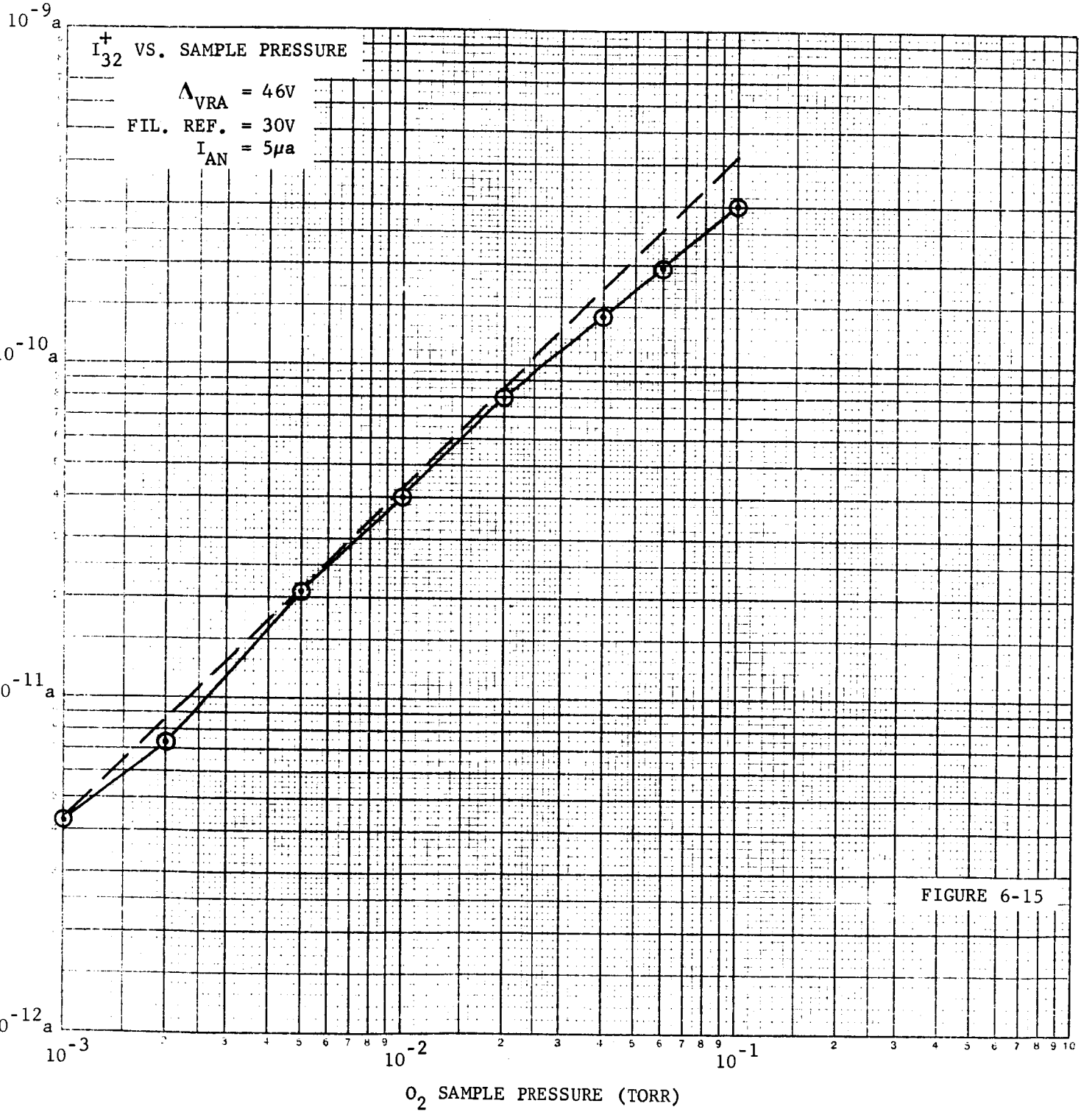
I_{32}^{+} VS. SAMPLE PRESSURE
Λ_{VRA} = 46V
FIL. REF. = 30V
I_{AN} = 5μa
10^{-9}a
10^{-10}a
10^{-11}a
10^{-12}a
10^{-3}
10^{-2}
10^{-1}
O_2 SAMPLE PRESSURE (TORR)

FIGURE 6-15

V (Filament Shield) = 217.6 volts

V (Ion Focus A) = 186.8 volts

V (Ion Focus B) = 201.8 volts

V (Anode) = 354.2 volts

V (Nozzle) = 0 volts

Emission Characteristics

V (Filament) = 2.44 volts

I^-_{TOTAL} = 165 microamperes

I^-_{ANODE} = 5 microamperes

I (Filament) = 1.35 amperes

It must be noted that when operating at the higher pressure levels the filament current, voltage and total emission are higher in order to maintain a constant anode current. When operating at the very high pressures this increased power reduces the filament strength so that the force due to the magnetic field causes the filament to drift away from the electron entrance aperture. Under test, it was necessary to reverse the filament polarity whereby the conditions returned to normal. Sustained operation at higher pressures required further polarity reversal.

7. CONCLUSION

The design analysis and fabrication of a high pressure magnetic ion source has been performed, resulting in a tested instrument capable of analyzing pressures within the ionizing region greater than 1×10^{-2} torr. Testing has shown that the ion source can operate up to 1×10^{-1} torr without too great a sacrifice in the output linearity. The ion source sensitivity for an air sample is approximately 7.5×10^{-9} amps/torr with 5 microamperes of ionizing electron current. The fabricated unit appears to realize the instrument goals in close agreement with the theoretical analysis. The other task requirements were to approach a sensitivity goal of 1×10^{-8} amps/torr and have a maximum time response of 30 milliseconds. A generated computer program has shown that the time constant of the ion source in an open configuration is 833 microseconds and will reach 95 percent of its final value (3 time constants) in 2.5 milliseconds.

It is recommended that a future effort be made to analyze the filament structure and mounting more thoroughly in order to strengthen the filament against the applied forces.

LIST OF REFERENCES

1. Guthrie, A. and Wakerling, R.K., Vacuum Equipment and Techniques, McGraw-Hill, New York, 1949, pp. 35, 36.

2. Cobine, J. D., Gaseous Conductors, Dover Publications, 1958

3. Brubaker, W.M., Influence of Space Charge on the Potential Distribution in Mass Spectrometer Ion Sources, J. App. Phys., Vol. 26, No. 8, August 1955

4. Spangenberg, K.R., Vacuum Tubes, McGraw-Hill, New York, 1948

5. Robinson, C.F., and Hall, L.G., Small General Purpose Cycloidal-Focusing Mass Spectrometer, Rev. Sci. Inst., Vol. 27, No. 7, July 1956

6. This material is fabricated and sold by the Hamilton Precision Metals Division of the Hamilton Watch Company.

7. Thomas and Skinner, Inc., Permanent Magnet Design, Bulletin M303, Indianapolis, Indiana

APPENDIX A

Analyzer System Time Response with Pump

```
C     P0=EXTERNAL PRESSURE
C     C0=INLET CONDUCTANCE
C     PS0=INITIAL SOURCE PRESSURE
C     VS=ION SOURCE VOLUME
C     CS=ION SOURCE CONDUCTANCE
C     PA0=INITIAL ANALYZER PRESSURE
C     VA=ANALYZER VOLUME
C     CA=ANALYZER CONDUCTANCE
C     SP=PUMPING SPEED
C     TS=TIME STEP
C     TCI=INLET TIME CONSTANT
C     TCS=ION SOURCE TIME CONSTANT
C     TCAI=ANALYZER TIME CONSTANT IN
C     TCA0=ANALYZER TIME CONSTANT OUT
C     PST=SOURCE PRESSURE AS F[T]
C     PAT=ANALYZER PRESSURE AS F[T]
      DIMENSION V[10]
   51 TYPE 52
   52 FORMAT[$ ENTER NUMBER OF VARIABLE TO BE CHANGED, I3,$,/
     1$ TYPE 11 FOR ALL CHANGES COMPLETE, $,/
     2$ TYPE 12 FOR ENTERING ALL NEW VALUES. $]
      ACCEPT 53,N
   53 FORMAT[I3]
      IF[N]51,54,55
   55 IF[N-11]56,57,1
   56 TYPE 58
   58 FORMAT[$ ENTER NEW VARIABLE VALUE, E10.3 $]
      ACCEPT 59, V[N]
   59 FORMAT[E10.3]
      GO TO 51
   57 P0 = V[1]
      C0 = V[2]
      PS0 = V[3]
      VS = V[4]
      CS = V[5]
      PA0 = V[6]
      VA = V[7]
      CA = V[8]
```

```
=     39          SP = V[9]
=     40          TS = V[10]
=     41          GO TO 54
=     42        1 TYPE 2
=     43        2 FORMAT[$ ENTER P0, C0, PS0, VS, CS, E10.3$]
=     44          ACCEPT 100, P0, C0, PS0, VS, CS
=     45      100 FORMAT[5E10.3]
=     46        3 TYPE 4
=     47        4 FORMAT[$ ENTER PA0, VA, CA, SP, TS,E10.3$]
=     48          ACCEPT 101,PA0, VA, CA, SP, TS
=     49      101 FORMAT[5E10.3]
=     50          V[1] = P0
=     51          V[2] = C0
=     52          V[3] = PS0
=     53          V[4] = VS
=     54          V[5] = CS
=     55          V[6] = PA0
=     56          V[7] = VA
=     57          V[8] = CA
=     58          V[9] = SP
=     59          V[10] = TS
=     60       54 PRINT 200, P0, C0, PS0, VS, CS, PA0, VA, CA, SP, TS
=     61      200 FORMAT[$ P0 = $,E10.3,$ C0 = $,E10.3,$ PS0 = $,E10.3,$ VS = $,
=     62         1E10.3,/$ CS = $,E10.3,$ PA0 = $, E10.3,$ VA = $,E10.3,$ CA = $,
=     63         2E10.3,/$ SP = $,E10.3,$ TS = $,E10.3///]
=     64          AK1 = C0/VS
=     65          AK2 = PS0
=     66          AK3 = CS/VS
=     67          AK4 = CS/VA
=     68          AK5 = AK4 + [1/VA]*[CA*SP/[SP+CA]]
=     69          AK6 = PA0
=     70          TCI = 1./AK1
=     71          TCS = 1./AK3
=     72          TCAI = 1./AK4
=     73          TCA0 = VA/[CA*SP/[SP+CA]]
=     74          PRINT 202,TCI,TCS,TCAI,TCA0
=     75      202 FORMAT[$ TCI = $,E10.3,$ TCS = $,E10.3,$ TCAI = $,E10.3,
=     76         1$ TCA0 = $,E10.3///]
=     77          AK7 = P0*AK1 + AK2*AK5 + AK3*AK6
```

```
=     78          AK8 = P8*AK1*AK5
=     79          AK9 = AK5 + AK1 + AK3
=     80          AK10 = AK1*AK5  + AK3*AK5 - AK3*AK4
=     81          IF[AK9*AK9-4.*AK10] 5,20,20
=     82        5 TYPE 6
=     83        6 FORMAT[$ SQ RT NEG, TRY NEW VALUES $]
=     84          GO TO 1
=     85       20 AK15 = [AK9/2.] - [[AK9*AK9]/4. - AK10]**.5
=     86          AK16 = [AK9/2.] + [[AK9*AK9]/4. - AK10]**.5
=     87          A= AK8/[AK15*AK16]
=     88          C=[1./[AK15-AK16]]*[AK7-[AK8/AK16]-[AK16*AK2]]
=     89          B= AK2-A-C
=     90          DO 30,N=1,200
=     91          T = TS*N
=     92          PST= A + B*EXP[-AK15*T] + C*EXP[-AK16*T]
=     93          PAT= A*AK4/AK5 + [[B*AK4/[AK15-AK5]]+[C*AK4/[AK16-AK5]]
=     94         1+AK6-A*AK4/AK5]*EXP[-AK5*T]-[B*AK4/[AK15-AK5]]*EXP[-AK15*T]
=     95         2-[C*AK4/[AK16-AK5]]*EXP[-AK16*T]
=     96          PRINT 203, PST, PAT, T
=     97      203 FORMAT[$ PST = $,E10.3,$ PAT = $, E10.3,$ T = $, E10.3]
=     98       30 CONTINUE
=     99          PRINT 204
=    100      204 FORMAT[$1$]
=    101          GO TO 51
=    102          END


PROGRAM ALLOCATION

  00037 V          00063 N          00064 P9         00066 C8
  00070 PS8        00072 VS         00074 CS         00076 PA8
  00100 VA         00102 CA         00104 SP         00106 TS
  00110 AK1        00112 AK2        00114 AK3        00116 AK4
  00120 AK5        00122 AK6        00124 TCI        00126 TCS
  00130 TCAI       00132 TCA8       00134 AK7        00136 AK8
  00140 AK9        00142 AK10       00144 AK15       00146 AK16
  00150 A          00152 C          00154 B          00156 T
  00160 PST        00162 PAT
```

SUBPROGRAMS REQUIRED

EXP

THE END

APPENDIX B

Analyzer System Time Response without Pump

```
C     P0=EXTERNAL PRESSURE
C     C0=INLET CONDUCTANCE
C     PS0=INITIAL SOURCE PRESSURE
C     VS=ION SOURCE VOLUME
C     CS=ION SOURCE CONDUCTANCE
C     PA0=INITIAL ANALYZER PRESSURE
C     VA=ANALYZER VOLUME
C     TS=TIME STEP
C     TCI=INLET TIME CONSTANT
C     TCS=ION SOURCE TIME CONSTANT
C     TCAI=ANALYZER TIME CONSTANT IN
C     PST=SOURCE PRESSURE AS F[T]
C     PAT=ANALYZER PRESSURE AS F[T]
      DIMENSION V[8]
   51 TYPE 52
   52 FORMAT[$ ENTER NUMBER OF VARIABLE TO BE CHANGED, I3,$,/
     1$ TYPE  9 FOR ALL CHANGES COMPLETE, $,/
     2$ TYPE 10 FOR ENTERING ALL NEW VALUES. $]
      ACCEPT 53,N
   53 FORMAT[I3]
      IF[N]51,54,55
   55 IF[N-9] 56,57,1
   56 TYPE 58
   58 FORMAT[$ ENTER NEW VARIABLE VALUE, E10.3 $]
      ACCEPT 59, V[N]
   59 FORMAT[E10.3]
      GO TO 51
   57 P0 = V[1]
      C0 = V[2]
      PS0 = V[3]
      VS = V[4]
      CS = V[5]
      PA0 = V[6]
      VA = V[7]
      TS = V[8]
      GO TO 54
    1 TYPE 2
    2 FORMAT[$ ENTER P0, C0, PS0, VS, CS, E10.3$]
```

```
=     39        ACCEPT 100, P0, C0, PS0, VS, CS
=     40    100 FORMAT[5E10.3]
=     41      3 TYPE 4
=     42      4 FORMAT[$ ENTER PA0, VA, T, E10.3 $]
=     43        ACCEPT 101,PA0, VA, T
=     44    101 FORMAT[3E10.3]
=     45        V[1] = P0
=     46        V[2] = C0
=     47        V[3] = PS0
=     48        V[4] = VS
=     49        V[5] = CS
=     50        V[6] = PA0
=     51        V[7] = VA
=     52        V[8] = TS
=     53     54 PRINT 200, P0, C0, PS0, VS, CS, PA0, VA, T
=     54    200 FORMAT[$ P0 = $,E10.3,$ C0 = $,E10.3,$ PS0 = $,E10.3,$ VS = $,
=     55       1E10.3,/$ CS = $,E10.3,$ PA0 = $, E10.3,$ VA = $,E10.3,$  T = $,
=     56       2E10.3]
=     57        AK1 = C0/VS
=     58        AK2 = PS0
=     59        AK3 = CS/VS
=     60        AK4 = CS/VA
=     61        AK5 = PA0
=     62        TCI = 1./AK1
=     63        TCS = 1./AK3
=     64        TCAI = 1./AK4
=     65        PRINT 202,TCI,TCS,TCAI
=     66    202 FORMAT[$ TCI = $,E10.3,$ TCS = $,E10.3,$ TCAI = $,E10.3///]
=     67        AK6 = P0*AK1 + AK2*AK4 + AK3*AK5
=     68        AK7 = P0*AK1*AK4
=     69        AK8 = AK4 + AK1 + AK3
=     70         AK9 = AK1*AK4
=     71        IF[AK8*AK8-4.*AK9]  5,20,20
=     72      5 TYPE 6
=     73      6 FORMAT[$ SQ RT NEG, TRY NEW VALUES $]
=     74        GO TO 1
=     75     20 AK10 = [AK8/2.]+[[AK8*AK8]/4.-AK9]**.5
=     76        AK11 = [AK8/2.]+[[AK8*AK8]/4.-AK9]**.5
=     77        A = AK7/[AK10*AK11]
```

```
      78          C = [1./[AK10-AK11]]*[AK6-[AK11*AK2]-[AK10*A]]
      79          B= AK2-A-C
      80          DO 30,N=1,200
      81          T = TS*N
      82          PST= A + B*EXP[-AK10*T] + C*EXP[-AK11*T]
      83          PAT=A+[B*AK4/[AK10-AK4]+C*AK4/[AK11-AK4]+AK5-A]*EXP[-AK4*T]
      84         1-[B*AK4/[AK10-AK4]]*EXP[-AK10*T]-[C*AK4/[AK11-AK4]]*EXP[-AK11*T]
      85          PRINT 203, PST, PAT, T
      86     203 FORMAT[$ PST = $,E10.3,$ PAT = $, E10.3,$ T = $, E10.3]
      87      30 CONTINUE
      88          PRINT 201
      89     201 FORMAT[$1$]
      90          GO TO 51
      91          END


PROGRAM ALLOCATION

  00033 V          00053 N          00054 PO         00056 CO
  0006C PSO        00062 VS         00064 CS         00066 PAO
  0007C VA         00072 TS         00074 T          00076 AK1
  00100 AK2        00102 AK3        00104 AK4        00106 AK5
  00110 TCI        00112 TCS        00114 TCAI       00116 AK6
  00120 AK7        00122 AK8        00124 AK9        00126 AK10
  00130 AK11       00132 A          00134 C          00136 B
  00140 PST        00142 PAT

UBPROGRAMS REQUIRED

  EXP
HE END
```